IN SITU VASCULAR REGENERATION USING SUBSTANCE P-IMMOBILISED POLY(L-LACTIDE-CO-ε-CAPROLACTONE) SCAFFOLDS: STEM CELL RECRUITMENT, ANGIOGENESIS, AND TISSUE REGENERATION

M. Shafiq,[1,2] Y. Jung, [1,2] S.H. Kim[1,2,3,*]

[1]Centre for Biomaterials, Biomedical Research Institute, Korea Institute of Science and Technology (KIST), 5, Hwarang-ro 14-gil, Seongbuk-gu, Seoul, 136-791, Republic of Korea.
[2]Department of Biomedical Engineering, Korea University of Science and Technology (UST) (305-350), Gajeong-ro, Yuseong-gu, Daejeon, Korea.
[3]NBIT, KU-KIST Graduate School of Converging Science and Technology, Korea University, Seoul, Korea

Abstract

In situ tissue regeneration holds great promise for regenerative medicine and tissue engineering applications. However, to achieve control over long-term and localised presence of biomolecules, certain barriers must be overcome. The aim of this study was to develop electrospun scaffolds for the fabrication of artificial vascular grafts that can be remodelled within a host by endogenous cell recruitment. We fabricated scaffolds by mixing appropriate proportions of linear poly (L-lactide-co-ε-caprolactone) (PLCL) and substance P (SP)-immobilised PLCL, using electrospinning to develop vascular grafts. Substance P was released in a sustained fashion from electrospun membranes for up to 30 d, as revealed by enzyme-linked immunosorbent assay. Immobilised SP remained bioactive and recruited human bone marrow-derived mesenchymal stem cells (hMSCs) in an *in vitro* Trans-well migration assay. The biocompatibility and biological performance of the scaffolds were evaluated by *in vivo* experiments involving subcutaneous scaffold implantations in Sprague-Dawley rats for up to 28 d followed by histological and immunohistochemical studies. Histological analysis revealed a greater extent of accumulative host cell infiltration and collagen deposition in scaffolds containing higher contents of SP than observed in the control group at both time points. We also observed the presence of a large number of laminin-positive blood vessels and Von Willebrand factor (vWF^+) cells in the explants containing SP. Additionally, scaffolds containing SP showed the existence of $CD90^+$ and $CD105^+$ MSCs. Collectively, these findings suggest that the methodology presented here may have broad applications in regenerative medicine, and the novel scaffolding materials can be used for *in situ* tissue regeneration of soft tissues.

Keywords: Stem cell, neo-vascularisation/angiogenesis, PLCL, substance P, electrospinning, vascular graft, tissue engineering/regenerative medicine, *in situ* tissue regeneration.

*Address for correspondence:
Dr. Soo Hyun Kim
Centre for Biomaterials, Biomedical Research Institute
Korea Institute of Science and Technology (KIST)
5, Hwarang-ro 14-gil, Seongbuk-gu
Seoul, 136-791, Republic of Korea
Telephone number: +82-2-958-5348
Fax number: +82-2-958-5308
E-mail: soohkim@kist.re.kr

Introduction

Vascular reconstruction remains a bottleneck clinical challenge for patients requiring coronary artery bypass, peripheral vascular surgery, or arteriovenous fistula. Over one million coronary revascularisation procedures are performed annually in the United States (Epstein *et al*., 2011). Despite their utility in the absence of autologous vessel replacements, conventional prosthetic vascular graft materials present a huge risk of thrombosis and infection (Zilla *et al*., 1994; Pektok *et al*., 2008). Alternatively, tissue engineering (TE) provides an attractive solution for vascular grafting by combining appropriate cell types and biomaterials, especially in the fabrication of small-diameter blood vessels (L'Heureux *et al*., 1998; Hoerstrup *et al*., 2006; Hashi *et al*., 2007). As a cell source, stem cells are most frequently used because of their self-renewal ability and multi-potency. Such tissue-engineered vascular grafts (TEVGs) have been shown to remodel within a host either by the direct differentiation of stem cells into vascular cell types or through the recruitment of host cells by paracrine mechanisms (Pittenger *et al*., 1999; Gimblem *et al*., 2007; Karp and Leng Teo, 2009). However, *ex vivo* manipulations of stem cells have drawbacks for clinical applications such as poor cell survival and safety of culture medium supplements (Chen *et al*., 2011).

To overcome these limitations, many researchers have tried to mimic endogenous wound healing processes by activating the host's own reparative capability (Askari *et al*., 2003; Schantz *et al*., 2007; Place *et al*., 2009; Hibino *et al*., 2011; Shao *et al*., 2012; Shafiq *et al*., 2015a). These studies suggested the possibility of tissue regeneration by recruitment of endogenous stem cells to defected regions without transplantation of exogenous cells. *In situ* tissue regeneration uses scaffolds alone or scaffolds combined with bioactive factors to create a microenvironment that allows the body's own cells to infiltrate and take over the scaffold and eventually integrate into native tissues (Lee *et al.,* 2010). For efficient and successful *in situ* tissue regeneration, an appropriate number of host stem cells must be recruited. While stem cells could be recruited into tissue-engineered scaffolds when implanted, the small infiltrating population might not be enough for *in situ* tissue regeneration (Heissig *et al*., 2002; Lee *et al*., 2008; Chen *et al.,* 2011; Nair *et al*., 2011; Wu *et al*., 2012). Researchers have also exploited the *in situ* tissue regeneration for the formation of blood vessels in synthetic and biodegradable vascular scaffolds (Cho *et al*., 2006; Yokota *et al*., 2008; Hibino *et al*., 2011; De Visscher *et al*., 2012; Roh *et al*., 2010; Yu *et al*., 2012; Lee *et al*.,

2013). A wide set of chemokines, including stromal cell-derived factor-1 alpha (SDF-1α) and granulocyte colony stimulating factor (G-CSF), have been employed *in vivo* to recruit endogenous mesenchymal stem cells (MSCs), haematopoietic stem cells (HSCs), endothelial progenitor cells (EPCs), and smooth muscle progenitor cells for the regeneration of tissues. However, these molecules are known to be easily cleaved or damaged by proteolytic enzymes. Additionally, such molecules cannot be easily processed or conjugated with scaffolds because of their high molecular weight. Therefore, alternative candidates such as cationic antimicrobial peptides, bioactive lipids, and short peptides are greatly desired for *in situ* TE (Hong *et al*., 2009; Shao *et a*l., 2012; Karapetyan *et al*., 2013).

Substance P (SP), an 11-amino acid neuropeptide is released by sensory nerve fibres during tissue insult or bone marrow (BM) damage and is involved in neuro-inflammation, cell proliferation, and wound healing (Nilsson *et el.,* 1985; Lotz *et al*., 1987; Hiramoto *et al*., 1998; Kim *et al*., 2014). It was previously reported that SP plays a novel role in mobilising MSCs from BM to wound sites, accelerating tissue repair. SP also possesses cellular and immune-modulatory effects and stimulates the production of various cytokines and growth factors, namely vascular endothelial growth factor (VEGF) and transforming growth factor-beta 1 (TGF-β), which can participate in a reparative process at the injury site (Hong *et al*., 2009; Kohara *et al*., 2010; Amadesi *et al*., 2012; Ko *et al*., 2012; Jin *et al*., 2015; Hong *et al*., 2015). These effects are expected by its local action, direct nerve innervation, direct cellular contact, and systematic effect through circulation. Noticeably, compared with other cytokines and growth factors, the injection of a very low dose of SP increased host cell mobilisation in peripheral blood (Hong *et al*., 2009). Moreover, in contrast to G-CSF, SP does not evoke any general pharmacological action or genetic toxicity and can be easily conjugated with biomaterials because of its small size (Momin *et al*., 1992; Hong *et al*., 2011; Kim *et al*., 2013). In view of the multifunctional nature of both angiogenic and chemotactic activities, the use of SP seems necessary to reduce side effects and minimise the cost of TE in translational approaches. Although SP has been shown to promote diabetic and non-diabetic wound healing, bone regeneration, and ischaemic revascularisation, to the best of our knowledge, its effect in vascular grafts has not been reported. We believe that the multifunctional cellular and immune-modulatory nature of SP could be very useful for the remodelling of vascular grafts through host cell recruitment, immune-modulation, and cell proliferation and/or differentiation.

The objective of this study was therefore to develop electrospun (ES) scaffolds for the fabrication of artificial vascular grafts that can be remodelled within the host through endogenous cell mobilisation and recruitment. To accomplish these goals, we examined the following criteria. First, for the graft material, we chose a mechano-elastic and biodegradable poly (L-lactide-co-ε-caprolactone) (PLCL, 50:50) copolymer because degradation is essential for host remodelling and mechanical conditioning is recognised as an important remodelling cue for vascular regeneration (Jeong *et al*., 2004; Hassan *et al*., 2011). Elastomers efficiently transduce mechanical stimulation to cells (Wu *et al.,* 2012). PLCL copolymers have been applied as biomaterials for vascular TE because of their high elasticity (Mun *et al*., 2012; Mun *et al.,* 2013). In addition, PLCL has potential applications as a scaffolding material in the regeneration of soft tissues, including blood vessels, tendons, skin, oesophagus, and cardiac tissues. Second, for host cell recruitment, we incorporated SP in scaffolds and provided long-term and sustained presence. Because of the degradation of SP by neutral endopeptidases and its short half-life *in vivo*, maintaining the persistence of SP following systematic administration is a challenge (Ko *et al.,* 2012; Kim *et al.,* 2014; Hong *et al*., 2014). To improve the *in vivo* stability, SP sequences have so far been either physically adsorbed or chemically attached onto scaffold surfaces (Ko *et al*., 2012; Kim *et al*., 2014; Kohara *et al*., 2010). The strategies employed for covalent attachment are time-consuming and involve several activation and coupling steps (Kim and Park, 2006). An alternative approach to enhance biochemical signals is the bulk modification of polymers prior to the fabrication step (Kuhl *et al*., 1996; Cook *et al*., 1997; Shafiq *et al*., 2015b). Our strategy relies on the direct conjugation of SP with the hydroxyl groups of the star-shaped PLCL (PLCL-SP). PLCL-SP may provide sustained release and localised presence of SP in scaffolds, recruit host cells, and could have immune-modulatory effects on the recruited cells within scaffolds. Third, to mimic extracellular matrix (ECM) architecture, we used ES since it enables the precise design of micro- and nanofibres. We varied the SP concentration to assess the host response to the vascular scaffolds containing different SP contents. To access biocompatibility and biological performance assessment, we implanted scaffolds subcutaneously in Sprague-Dawley (SD) rats ($n = 16$) for up to 28 d and performed histological and immunohistochemical studies. PLCL-SP can be processed to fabricate different ready-to-use shapes, such as membranes, scaffolds, and vascular grafts depending upon the final application of these materials for the *in situ* regeneration of soft tissues, such as blood vessels, tendons, skin, oesophagus, and bladder (Fig. 1A).

Materials and Methods

Materials

L-lactide was purchased from PURAC Biomaterials (Seoul, Korea) and recrystallised in ethyl acetate before polymerisation. Caprolactone, 1-dodecanol (reagent grade, purity = 98 %), tin (II) bis (2-ethylhexanoate) ($Sn(Oct)_2$, purity ≥ 99 %), N,N-dimethylformamide (DMF, purity ≥ 99.8 %), formamide (purity ≥ 99.5 %), dimethylsulphoxide (DMSO, purity ≥ 99.5 %), Dulbecco's phosphate-buffered saline (D-PBS), formalin solution (neutral buffered 10 %), 1,1'-carbonyldiimidazole (CDI; reagent grade), tripentaerythritol (TPE, technical grade), anhydrous dichloromethane (DCM), and ethanol were purchased from Sigma Aldrich (Seoul, South Korea). 1,1,1,3,3,3-hexafluoro-2-propanol (HFIP, purity = 99 %) was purchased from Tokyo Chemical Industry (Tokyo, Japan). Caprolactone was purified

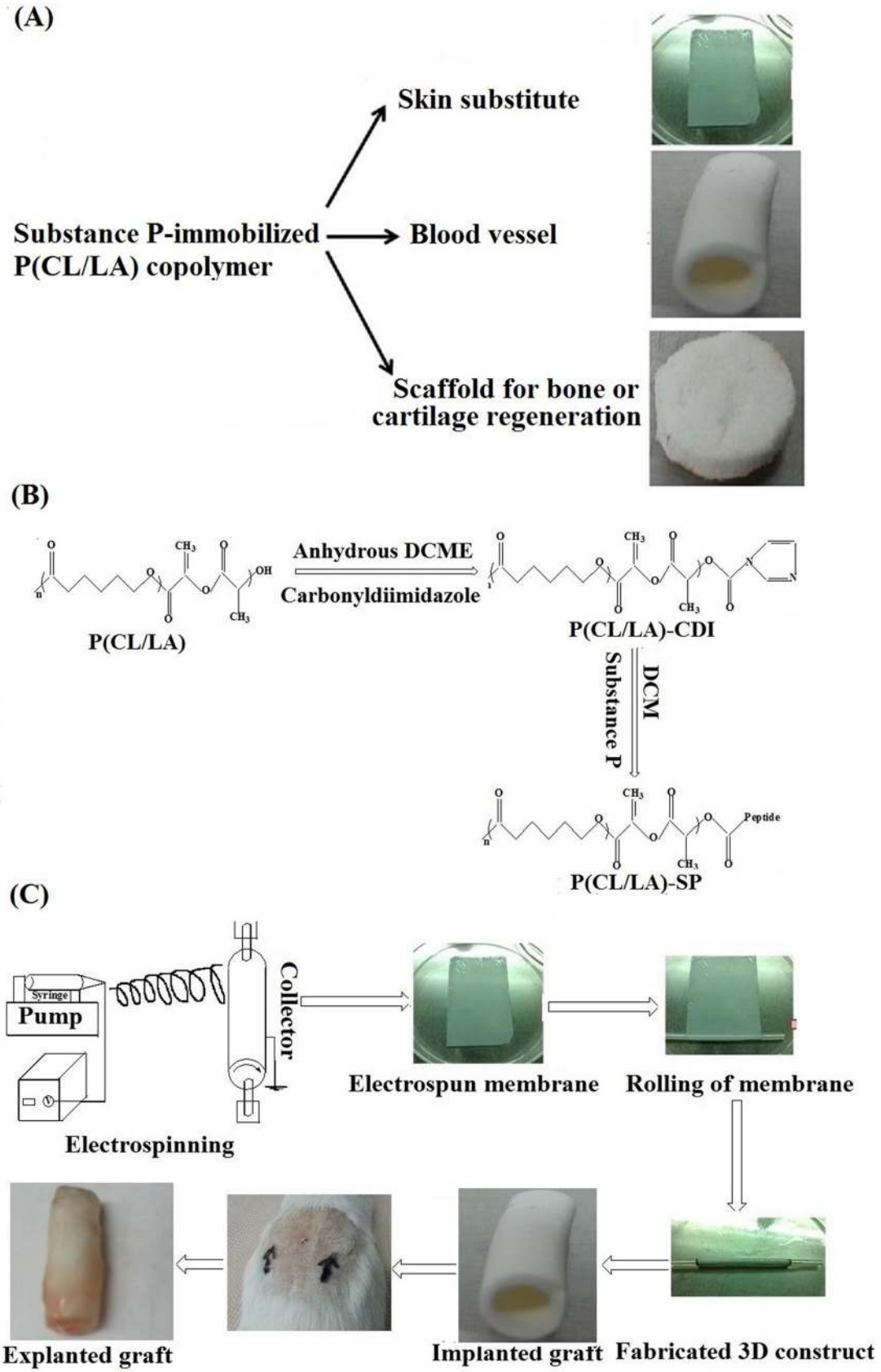

Fig.1. (**A**) Schematic illustration of the key applications of SP-immobilised PLCL copolymers. PLCL-SP copolymers can be used to fabricate skin substitutes, artificial blood vessels or scaffolds for bone and cartilage regeneration. (**B**) Conjugation of SP with star-shaped PLCL copolymer. The hydroxyl groups of PLCL copolymer were activated with 1,1'-carbonyldiimidazole (CDI) and reacted with the NH_2 groups of SP. (**C**) Schematic illustration of the designed study. We fabricated electrospun nanofibres by mixing appropriate proportions of linear PLCL and star-shaped PLCL-SP and developed vascular scaffolds (inner diameter = 4 mm, wall thickness = 200 μm) using a scaffold-membrane approach. Vascular grafts were implanted subcutaneously in Sprague-Dawley rats (n = 16) for up to 28 d and characterised for host cell infiltration, extracellular matrix deposition, stem cell recruitment, and angiogenesis.

using 4,4'-methylenebis(phenyl isocyanate) by fractional distillation. Collagen type 1A (BD, Franklin Lakes, NJ, 3 mg/mL) was used after dilution with the appropriate amount of acetic acid. SP (RPKPQQFFGLM-NH_2) (> 95 % purity) was purchased from Peptron (Daejeon, Republic of Korea). Chloroform ($CHCl_3$) and methanol (CH_3OH, purity ≥ 99.5 %) were purchased from Daejung Chemical and Metal Co. Ltd (Daejeon, Republic of Korea) and used without further purification. $Sn(Oct)_2$ was distilled under reduced pressure and dissolved in dry toluene.

Synthesis of linear and eight-arm PLCL copolymers

Linear and star-shaped PLCL (50:50) copolymers were synthesised by ring opening polymerisation, as described in detail in our previous reports, with slight modifications (Mun *et al*., 2012; Shafiq *et al.*, 2015b). Briefly, 1-dodecanol and TPE were used as initiators to synthesise linear and star-shaped PLCL copolymers. Polymerisation was carried out in bulk in a 250 mL glass ampoule containing 100 mM L-lactide (LA), 100 mM ε-caprolactone (CL), 0.5 mM initiator, and 1.0 mM $Sn(Oct)_2$. The ampoule was purged three times with nitrogen (N_2) and subjected to vacuum for 6 h. The sealed ampoule was then transferred to a pre-heated silicon oil bath (145 °C), and polymerisation was carried out for 24 h with mild stirring. The resultant copolymers were then dissolved in $CHCl_3$, filtered through a 4.5 μm pore membrane, and precipitated into an excess of CH_3OH.

Conjugation of SP with star-shaped PLCL copolymer

SP was conjugated with eight armed star-shaped PLCL copolymers, as previously described, with slight modifications (Fig. 1B) (Shafiq *et al*., 2015b). Briefly, star-shaped PLCL (M_n ~ 67382, PDI = 1.80, 4.48×10^{-5} moles) copolymer was dissolved in anhydrous DCM (10 mL) with continuous stirring under N_2 atmosphere for 2 h. Once PLCL was dissolved, CDI (7.16×10^{-4} moles) dissolved in anhydrous DCM (2 mL) was added, and the reaction was continued for 6 h under N_2 atmosphere. PLCL-CDI was precipitated using excess ethanol and contents were dried in a vacuum oven for 48 h at room temperature. PLCL-CDI (1.48×10^{-5} moles) was dissolved in anhydrous DCM and stirred for 3 h under N_2 atmosphere. SP (1.86×10^{-6} moles) was dissolved in anhydrous DMSO and poured into the stirring PLCL-CDI solution (pH 8.2). The reaction was continued for 24 h at ambient temperature (25 °C). SP-conjugated star-shaped PLCL copolymers were precipitated with excess ethanol, washed with three times PBS, and dried in a vacuum oven at ambient temperature for 3 d. The vacuum-dried copolymer was stored at -20 °C for subsequent use.

Preparation of electrospun nanofibres

In this study, two types of electrospun mats were prepared by ES: PLCL and PLCL/PLCL-SP (SP content = 16.4, 33.3, and 49.7 nmol/g of the mesh). Briefly, to fabricate PSP-17 membrane, 966 mg of PLCL (Mn = 198 kDa, PDI = 1.90) and 34 mg of PLCL-SP copolymers were added. For PSP-34, and PSP-50 membranes, 69.1 mg and 103 mg of PLCL-SP copolymers were added, respectively. Noticeably, one mg of PLCL-SP copolymer contains 0.4827 nmol of SP as evaluated by amino acid analysis (Shafiq *et al*., 2015b). PSP-17, PSP-34, and PSP-50 identification codes have been used in the manuscript, which correspond to 16.4, 33.3, and 49.7 nmol/g of SP in the mesh, respectively. Electrospinning was performed by a custom-made ES setup using the following conditions: 9 % w/v solution in HFIP, needle-collector distance of 18 cm, flow rate of 1 mL/h, voltage of 18 kV, and a 21-gauge needle. The needle was clamped to the positive electrode of a high voltage power supply, and the negative electrode was connected to a rotating aluminium drum collector (250 rpm). Solution was delivered using a syringe pump (ESP200D, NanoNC). Electrospun nanofibres were dried in a vacuum oven at ambient temperature for 3 d, and stored in a desiccator for subsequent use.

Characterisation of PLCL and PLCL-SP copolymers

Gel permeation chromatography

The molecular weight of linear and star-shaped PLCL copolymers was analysed by gel permeation chromatography (Viscotek GPCmaxVE 2001, Houston, TX, USA) equipped with micro-styragel columns calibrated with polystyrene. Chloroform was used as the mobile phase, with a flow rate of 1.0 mL/min at 40 °C.

Amino acid analysis

To evaluate the conjugation of SP with star-shaped PLCL copolymers, amino acid composition analysis was carried out according to previously published protocol (Chun *et al.,* 2009; Shafiq *et al*., 2015b). Briefly, the conjugate sample was dissolved in $CHCl_3$ and then dried for hydrolysis. Samples were hydrolysed in 6 N hydrochloric acid at 110 °*C for 24* h, and then derived by phenylisothiocyanate (20 *μL of methanol:* water: triethylamine: phenylisothiocyanate in the ratio 7:1:1:1). After micro-centrifugation of the derived conjugate sample, supernatant was filtered with a 0.45 mm filter and analysed by a high-pressure liquid chromatography (HPLC) equipped with a C18 column (Waters Nova-Pak C18, 3.9 × 300 mm, 4 *μ*m), oven (46 °*C), injector (HP 1100 series, Auto* sampler), pump (HP 1100 series, binary pump), and variable wavelength detector (HP 1100 series). The solvent system (solvent A: 140 mM sodium acetate buffer, 0.15 % triethylamine, 6 % acetonitrile, 0.03 % ethylenediaminetetraacetic acid (EDTA), pH 6.1 and solvent B: 60 % acetonitrile, 0.015 % EDTA) consisted of the linear gradient (0-100 %) of solvent B. The samples were detected at 254 nm at the flow rate of 0.4 mL/min and injection volumes of 2 *μ*L for a standard curve, and 10 *μL for samples, to determine the amounts of each amino acid. Mole fraction of each amino acid* was calculated by comparing with the peak area from standard (250 pmol).

Morphological analysis of electrospun nonwoven meshes

The morphology of ES nonwoven meshes was characterised by field emission scanning electron microscope (Hitachi S-4200, Hitachi High-Technologies, Tokyo, Japan). All samples were sputter coated with gold prior to analysis. The diameter of the fibres was calculated using Image J and presented as mean ± standard deviation of 70 fibres.

In vitro release kinetics of SP from electrospun nonwoven meshes

To analyse the release kinetics of SP from PLCL/PLCL-SP meshes, samples (n = 3, area = 1 × 1 cm^2) were placed in 50 mL plastic tubes, and 600 μL of release medium (0.1 % bovine serum albumin in PBS) was added to each tube (Lee *et al.,* 2012). Samples were incubated at 37 °C with shaking at 100 rpm up to 30 d. At pre-determined time points, media were collected and replaced with fresh media to provide infinite sink conditions to the samples. The cumulative amount of SP released to the media was evaluated using a SP enzyme-linked immunosorbent assay (ELISA) Development Kit (R&D Systems, Minneapolis, MN, USA) following the manufacturer's instructions.

In vitro Trans-well migration assay

The migratory response of human MSCs (hMSCs) (passage 6) towards PLCL, SP, and PLCL/PLCL-SP was analysed using Millipore QCM™ 24-well cell migration assay (ECM508, Millipore, Billerica, MA) following manufacturer's instructions with slight modifications (Kim *et al*., 2014). Human MSCs (Centre for Regenerative Medicine, Texas A&M University, College station, TX, USA) were expanded at 37 °C, 5 % CO_2 in Dulbecco's Modified Eagle Medium (Life technologies, Waltham, MA) supplemented with foetal bovine serum (10 %) and penicillin/streptomycin (1 %) and passaged at 70 % confluence using 0.25 % Trypsin-EDTA (Invitrogen) (Phadke *et al*., 2013). Collagen type 1A (BD, Franklin Lakes, NJ; 0.1 mg/mL in acetic acid) was added in the inserts and the plate was incubated at 37 °C with 5 % CO_2 for 2 h.

After washing three times with PBS, 300 μL of cell suspension (1 × 104 cells) in serum-free medium was added to the inserts. Cells were homogenised for 48 h in an incubator (Kim *et al*., 2015). About 250 μL of SP solution (0.1 mg/mL in deionised water), PLCL or PLCL/PLCL-SP nonwoven meshes (diameter = 15 mm, weight ~ 1.5 mg) were placed in the wells. About 500 μL of the media was added in the inserts, and the Trans-well plate was incubated at 37 °C for 48 h. Following manufacturer's instructions, inserts were washed and cells were stained. Cells were observed using light microscopy (Eclipse TE2000U; Nikon, Tokyo, Japan).

Fabrication of vascular scaffolds

Nonwoven meshes were treated with 70 % ethanol overnight, and then dried for 2 d at room temperature. The dried nonwoven meshes were sterilised using ethylene oxide gas at 1.0 bar and 35 °C (E.O Gas Sterilizer, PERSON-E035/50, PERSON Medical, Korea). The sterilised meshes were coated with collagen solution (1 mg/mL in acetic acid) and incubated at 4 °C overnight (Mun *et al*., 2012). To remove residual solution, collagen-coated meshes were washed three times with PBS. Vascular scaffolds (inner diameter = 4 mm, wall thickness ~ 200 μm) were fabricated from membranes using a scaffold-membrane approach, whereby membranes were rolled around a sterilised silicon tube ten times (Fig. 1C) (Mun *et al*., 2012). About 5 μL of fibrin gel was used to join the layers only at the 2nd and 10th layer of the scaffolds.

Implantation of scaffolds

All animals were treated in accordance with the recommendations for handling of laboratory animals for biomedical research compiled by the committee on the safety and ethical handling regulation for laboratory experiments at Korea Institute of Science and Technology and Seoul National University, Republic of Korea. Male, Sprague-Dawley rats (age = 7 weeks, weight = 200-250 g, n = 16) were obtained from Orient Bio INC (Gyeonggi, Republic of Korea) and randomly divided into four experimental groups to receive PLCL or PLCL/PLCL-SP vascular grafts for 14 or 28 d. Four samples were implanted *per* group. Animals were anaesthetised with isoflurane (2 % for the induction and 1 % for the maintenance) and a single dose of 5 mg/100 g ketamine IM. Under aseptic conditions, a longitudinal incision was made in the dorsal skin of the rats, and a muscle pocket was created using blunt scissors, without injuring the deep muscle. Scaffolds were implanted in the space between the skin and deep muscle. Two samples were implanted *per* animal on the right and left side of the incision, and the skin was sutured using 3-0 cm silk sutures. After 14 or 28 d, animals were sacrificed, and samples were explanted. Because easy isolation of the surrounding tissues from the samples was not possible, the vascular grafts along with the surrounding tissues were explanted. The explanted samples were fixed in 10 % formalin for 24 h, embedded in a mixture of paraffin and ethylene vinyl acetate (5:1) and stored at −20 °C for analysis. Paraffin blocks were sectioned into slices (thickness = 6 μm) for histological and immunofluorescence staining.

Characterisation of explanted grafts

Histological analysis of the explanted grafts

The cell infiltration and tissue regeneration abilities of the retrieved scaffolds were assessed using histological examination. Histological analysis of the retrieved grafts was carried with haematoxylin and eosin staining and Masson's trichrome (MT) staining using standard protocols (Go *et al*., 2008; Choi *et al*., 2008). With MT staining, connective tissues were stained blue, nuclei were stained dark red/purple, and cytoplasm was stained red/pink. The stained sections were observed by light microscopy (Eclipse TE2000U; Nikon, Tokyo, Japan). The dashed lines in Fig. 4 (as well as in subsequent figures) represent the boundaries between the surrounding tissues and the scaffolds, whereas "*L*" represents lumen of the graft.

Evaluation of angiogenesis and stem cell recruitment in vivo

For immunostaining, anti-CD90/CD105 antibody, mouse anti-rat CD68 antibody (MCA341R, AbD Serotec, NC, USA), rabbit anti-von Willebrand Factor antibody (vWF, Abcam, Cambridge, MA, USA), and anti-laminin antibody (Sigma Aldrich, ST. Louis, MO, USA) were used. Paraffin sections were deparaffinised, rehydrated, and blocked using 4 % BSA in PBS for 1 h at room temperature. For CD90 and CD105 immunostaining, the sections were incubated with anti-CD90 antibody (1:400 dilution) and anti-CD105 antibody (1:200 dilution) diluted with blocking serum at room temperature for 2 h, washed with PBS three times,

and then treated with Alexa 488-conjugated goat anti-mouse antibody or Alexa 594-conjugated goat anti-rabbit antibody (1:400 dilution; Invitrogen). For staining cellular nuclei, 4',6-diamidino-2-phenylindole (DAPI; 1:1000, Life Technologies, Carlsbad, CA, USA) was applied before confocal imaging. For laminin immunostaining, sections were incubated with the rabbit anti-laminin antibody (1:25 dilution), followed by Alexa 594-conjugated goat anti-rabbit antibody. As described, this was followed by DAPI for nuclear staining. Similar procedure was followed for the immunostaining of vWF and CD68. For vWF staining, the sections were incubated with vWF antibody (1:400 dilution), followed by Alexa Flour 594 conjugated goat anti-rabbit antibody (1:200). For CD68 staining, sections were incubated with mouse anti-rat CD68 antibody (1:100) followed by Alexa Flour 594 conjugated rabbit anti-mouse antibody (1:200). The stained sections were observed using fluorescence microscopy (Eclipse TE2000U; Nikon, Tokyo, Japan). The numbers of positive cells were counted in three randomly selected images from both the interior and periphery regions of the retrieved scaffolds. The counts were averaged and are presented as means ± SD. For blood vessel quantification, the confocal images (laminin-positive cells or blood vessels) were analysed with Image J software (U.S. National Institutes of Health, Bethesda, MD, USA) using the "analyze particle".

Statistical analysis

All quantitative results were obtained from at least three samples for analysis using Image J 1.43 (National Institute of Mental Health, Bethesda, MD, Image Pro version 4.5, Media Cybernetics, Silver Spring, MD, USA). Data were expressed as the mean ± standard deviation. A two-tailed student's *t*-test was used to compare data from different groups. A value of $p < 0.05$ was considered statistically significant.

Results

Linear PLCL and PLCL-SP were synthesised using our previously published article and the purity was confirmed (Jeong *et al*., 2004; Shafiq *et al.*, 2015a).

Morphology of electrospun non-woven meshes

Nanofibres were fabricated by electrospinning PLCL and PLCL-SP copolymer blends onto a rotating mandrel. Morphology of the fibres and dimensions were characterised by SEM. Scanning electron microscopy images of electrospun mats are shown in Fig. 2, revealing the non-woven nanofibrous morphology of PLCL as well as PLCL/PLCL-SP meshes with interconnected pores. Uniform, continuous, and smooth nanofibres without bead defects and exhibiting a well-defined morphology were formed. PLCL nanofibres (the control group) showed uniform morphology and smooth surfaces. Moreover, fibre size was uniform, and no fusion was observed among the fibres. The average diameter of the fibres was 1.077 ± 0.181 μm. The PLCL/PLCL-SP meshes were also homogeneous and uniform in size. In addition, no adherence was observed between the nanofibres. The average diameter of PSP-17, PSP-34, and PSP-50 fibres was 0.690 ± 0.098 μm, 0.604 ± 0.092 μm, and 0.502 ± 0.100 μm, respectively (Fig. 2b).

***In vitro* release kinetics of Substance P from non-woven meshes**

The *in vitro* release profile of SP from the electrospun mats ($n = 3$) was measured using ELISA kit (Fig. 3a, b). Electrospun mats containing covalently conjugated SP showed a cumulative release of 1389.3 ± 60.7 pg/mL (PSP-17), 1434.9 ± 42.4 pg/mL (PSP-34), and 1351.8 ± 40.3 (PSP-50) of SP over 30 d (Fig. 3a). These values correspond to 2.05 ± 0.19, 0.93 ± 0.19, and 1.00 ± 0.11 % of the initially loaded SP released from the PSP-17, PSP-34, and PSP-50 meshes, respectively, during this time point (Fig. 3b).

***In vitro* Trans-well migration assay**

The ability of SP, PLCL, and PLCL/PLCL-SP to induce chemotaxis towards hMSCs was evaluated using an *in vitro* Trans-well migration assay. The results confirmed that many cells migrated through the membrane pores by the action of soluble SP or PLCL/PLCL-SP mats compared with the control group (Student's *t*-test, $p < 0.05$). As shown in Fig. 3, only few cells migrated to the lower part of the membrane in the control group. By contrast, significantly greater number of cells migrated (Student's *t*-test, $p < 0.05$) to the lower surface of membrane in response to SP. PLCL/PLCL-SP meshes also significantly ($n = 6$, $p < 0.05$) induced the migration of hMSCs to the lower part of the membrane compared with the control group. The numbers of migrated cells were quantified and the graph was shown in Fig 3c. The numbers of migrated cells were as follows: PLCL, 15.33 ± 2.88; PSP-17, 20.8 ± 2.98; PSP-34, 41.8 ± 4.38; PSP-50, 57.8 ± 4.02; SP, 68.1 ± 6.69 (Fig. 3c). It was observed that meshes containing higher content of SP recruited more cells. These results demonstrated that the bioactivity of SP was preserved, which may be a critical factor for *in vivo* application and evaluation.

Characterisation of explanted grafts

Haematoxylin and eosin staining

After 14 or 28 d of implantation, the scaffolds had adhered to the surrounding or subcutaneous tissues. The representative micrographs of histological sections of explanted samples are shown in Fig. 4. Both scaffold types showed an increase in cell infiltration with implantation time. The sections showed regeneration of vascular tissues and infiltration of host cells. In the control and PSP-17 groups, cells only slightly infiltrated into the grafts, which were mainly confined at the tissue-scaffold boundary 14 d after implantation (Fig. 4a, b). Moreover, granular tissues were observed near the tissue-scaffold interface in these groups. The interior portion of the PLCL graft was devoid of cells, whereas, few cells were seen in the inner site of the PSP-17 graft. By contrast, cell infiltration in the PLCL/PLCL-SP scaffolds (PSP-34 and PSP-50) was much more pronounced 14 d after implantation (Fig. 4c, d). In these groups, infiltrating cells were observed throughout the cross-section of the grafts and homogeneously distributed within the graft wall, and granular tissues were formed (Fig. 4c, d). For the 28-day implantation, only few cells

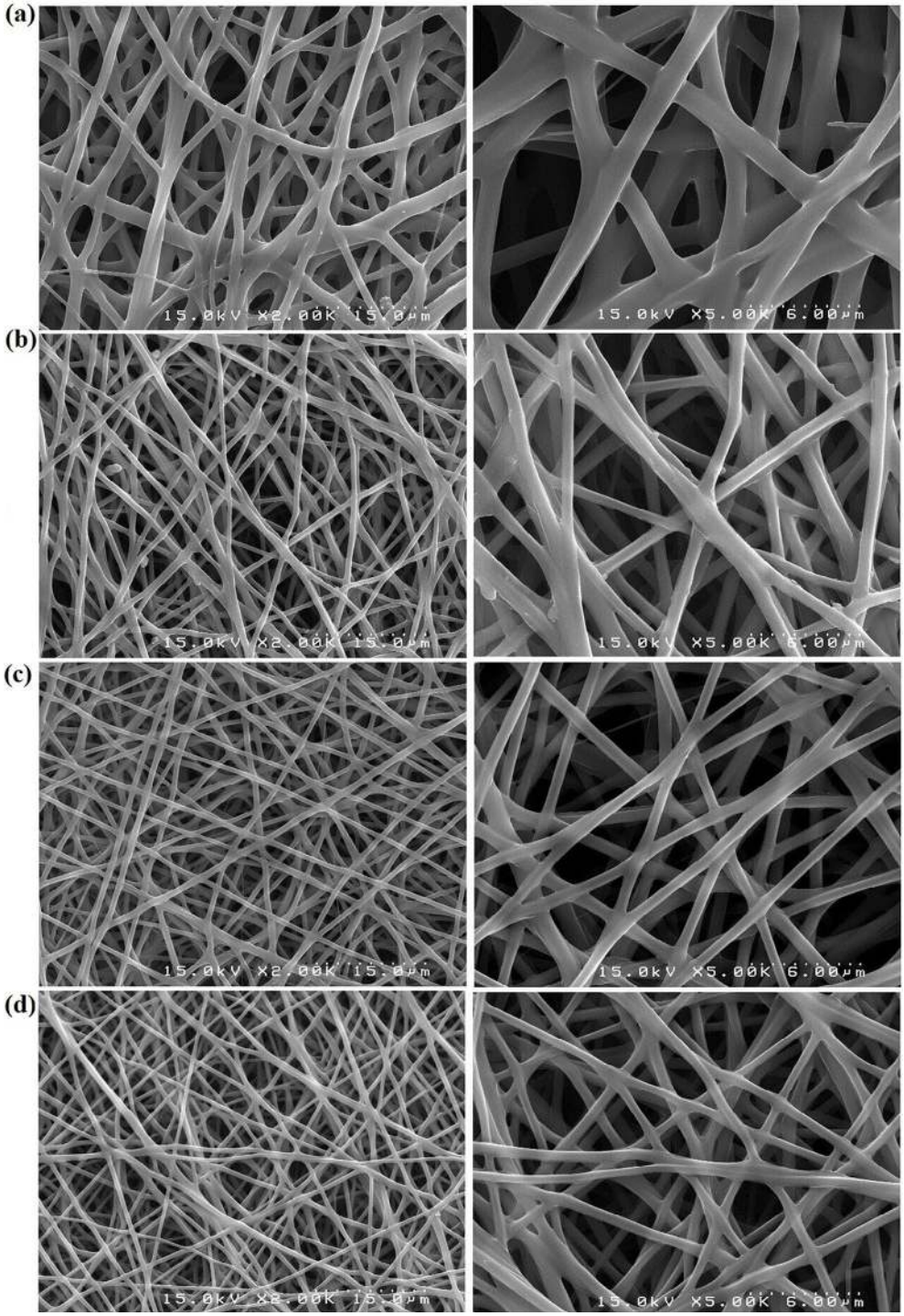

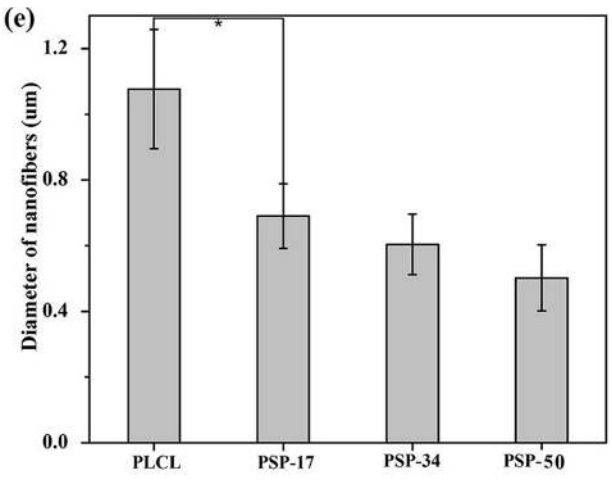

Fig.2. Morphology of nanofibrous scaffolds. (**a-d**) FE-SEM photomicrographs of electrospun PLCL and PLCL/PLCL-SP nanofibres. Smooth and homogenous nanofibres were formed. Left panel, Scale bars = 15.0 μm; right panel, Scale bars = 6.0 μm. (**e**) Average diameter of nanofibres computed from FE-SEM micrographs. The average diameter of PLCL, PSP-17, PSP-34, and PSP-50 nanofibres was 1.0766 ± 0.181, 0.690 ± 0.098 μm, 0.604 ± 0.092 μm, and 0.502 ± 0.100 μm, respectively. * = significantly different from other groups, $p < 0.05$, Student's *t*-test, data are expressed as mean ± SD for $n = 6$.

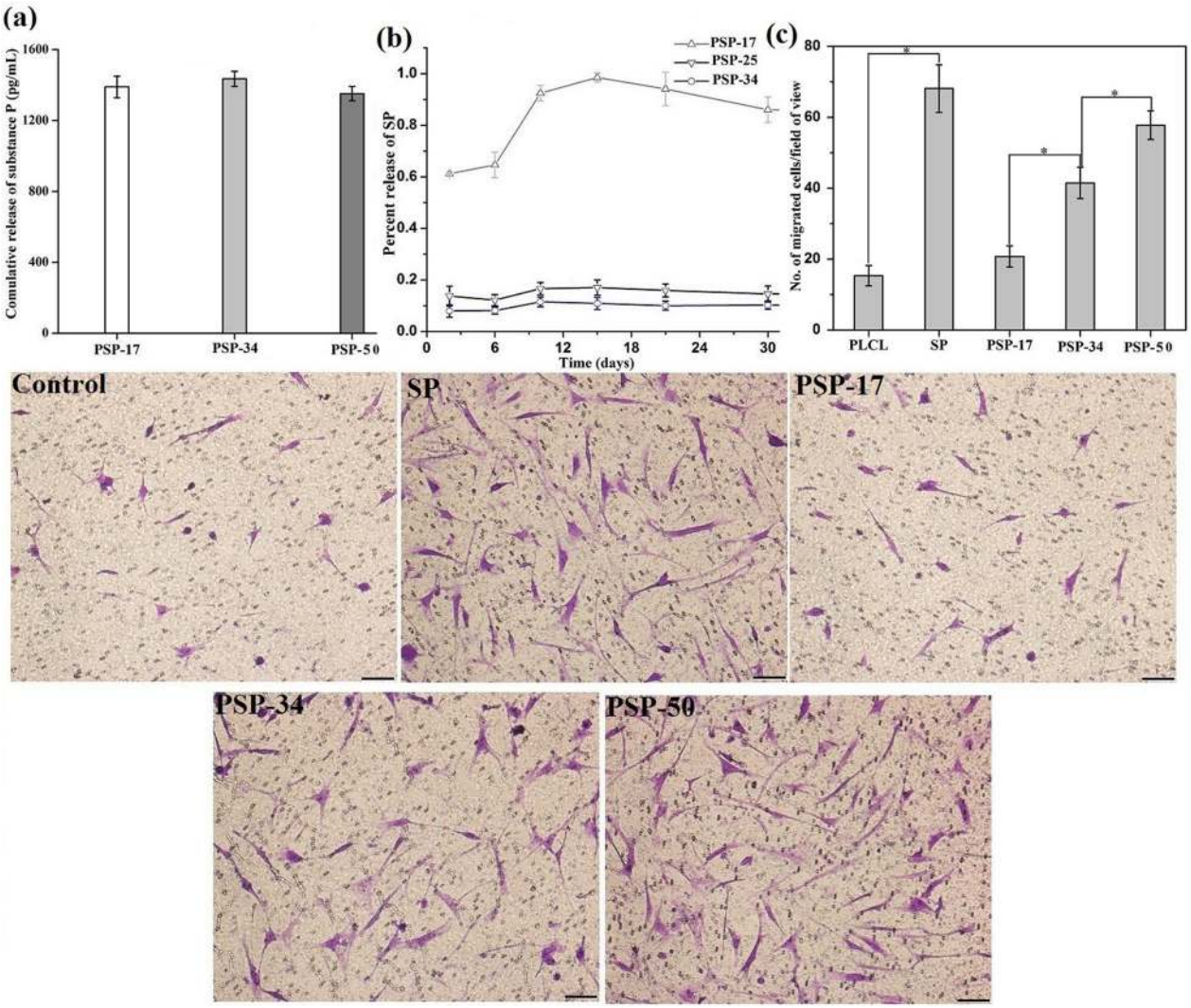

Fig. 3. Sustained release of SP from nanofibrous scaffolds and an *in vitro* Trans-well migration assay. (**a**-**b**) Sustained release of SP from PLCL/PLCL-SP scaffolds as quantified by ELISA. (**a**) Cumulative release of SP from scaffolds. A total 1389.3 ± 60.7, 1434.9 ± 42.4, and 1351.8 ± 40.3 pg/mL of SP was released from scaffolds over 30 d. (**b**) Percentage release of SP from the meshes over 30 d. A total 2.05 ± 0.19 %, 0.93 ± 0.19 %, and 1.00 ± 0.11 % of the initially loaded SP was released from the PSP-17, PSP-34, and PSP-50 meshes, respectively over a period of 30 d. Data are expressed as mean ± S.D for $n = 6$. (**c**) Graph showing the number of migrated cells *per* field of view in an *in vitro* cell migration assay. SP and PLCL/PLCL-SP nanofibres effectively recruited MSCs. * = significantly different from other groups, $p < 0.05$, Student's *t*-test, data are expressed as mean ± SD for $n = 6$. Rows 2 and 3): *In vitro* migration of MSCs toward PLCL, SP, and PLCL/PLCL-SP nanofibres. Scale bars, 100 μm.

existed in the central region of the control, whereas significantly more cells were found in the central region of the PSP-17 and PSP-34 scaffolds. The significantly more homogeneous cell infiltration in the bulk of the PLCL/PLCL-SP vascular scaffolds implanted for 28 d may be attributed to the gradual migration and proliferation of infiltrating host cells. Consequently, granular tissues were formed to a large extent in these SP groups. PSP-50 showed less cellularity at this time point. Several categories of host cells such as fibroblasts, myofibroblasts, vascular cells, and macrophages may have infiltrated into the grafts from the adjacent tissues or arteries (as described in the next sections). We also assessed inflammatory response to these scaffolds and found that only few $CD68^+$ cells were accumulated in the control and SP groups at both time points.

Histology of scaffolds implanted in vivo

Collagen was detected in the bulk of control and PLCL/PLCL-SP scaffolds implanted for 14 d and 28 d (Fig. 5). Collagen deposition was observed in the PLCL scaffolds implanted for 14 d, suggesting that the infiltrating fibroblasts remained viable and functional, contributing to the regeneration of neotissues (Fig. 5a). On the other hand, the PSP-17 scaffold showed less deposition of collagen compared with the control group at this time point, which was attributed to the low numbers of infiltrated cells (Fig. 5b). Collagen fibres were observed throughout the cross-section of PSP-34 and PSP-50 scaffolds after 14 d of implantation (Fig. 5c, d). Control, PSP-17, and PSP-34 grafts explanted 28 d after implantation showed a large amount of collagen deposition compared with grafts retrieved 14 d after implantation (Fig. 5). PSP-50 showed

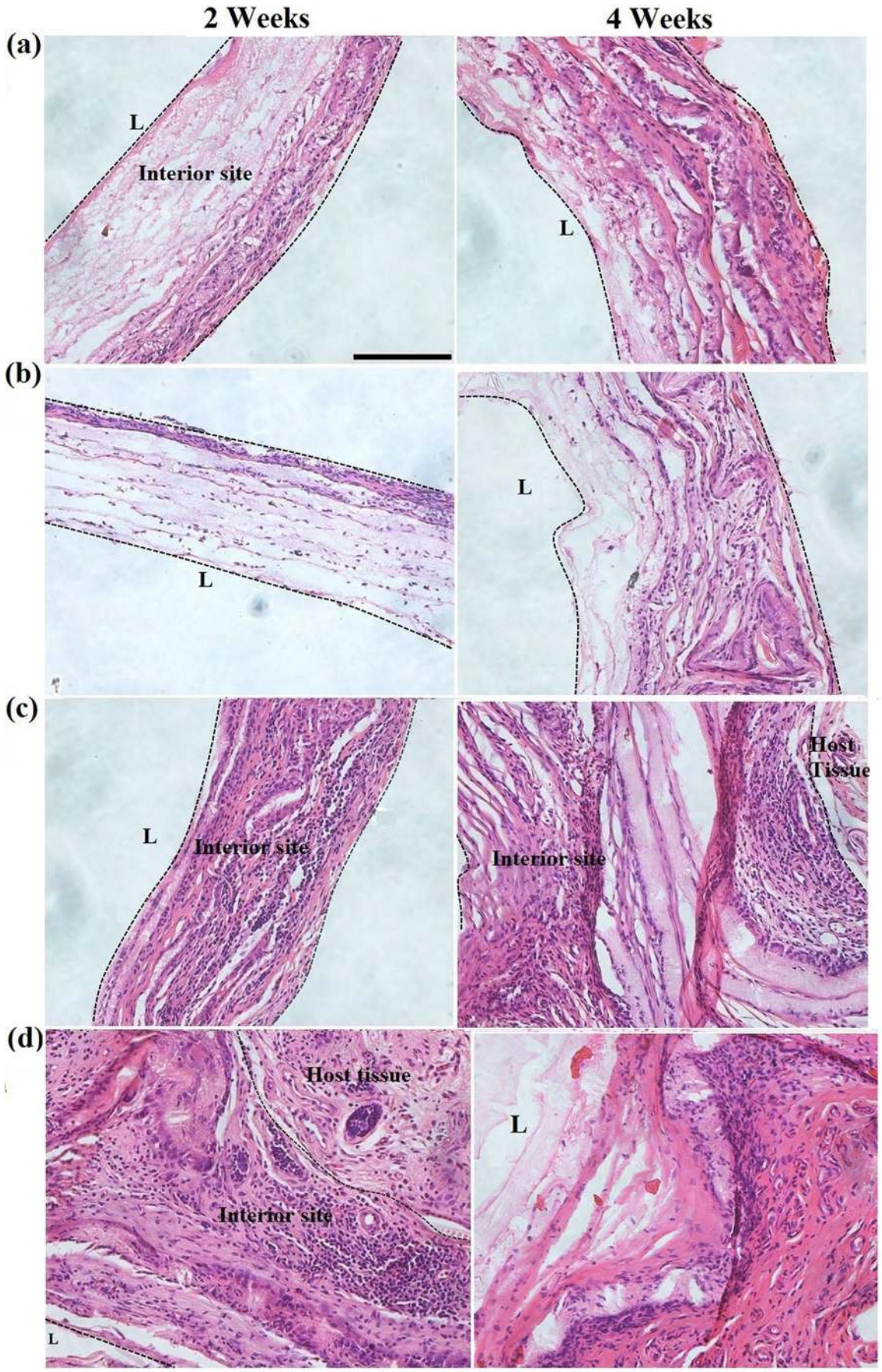

Fig. 4. Histological images of retrieved scaffolds 2 weeks and 4 weeks after implantation. (**a**) Control; (**b**) PSP-17; (**c**) PSP-34; and (**d**) PSP-50. Dashed lines represent the boundaries between surrounding tissues and scaffolds. "L" represents lumen of samples. Left and right panels show 2-weeks and 4-weeks groups, respectively. PSP-34 and PSP-50 showed the highest amount of host cell infiltration than that of other groups at both time points. Scale bars, 100 μm.

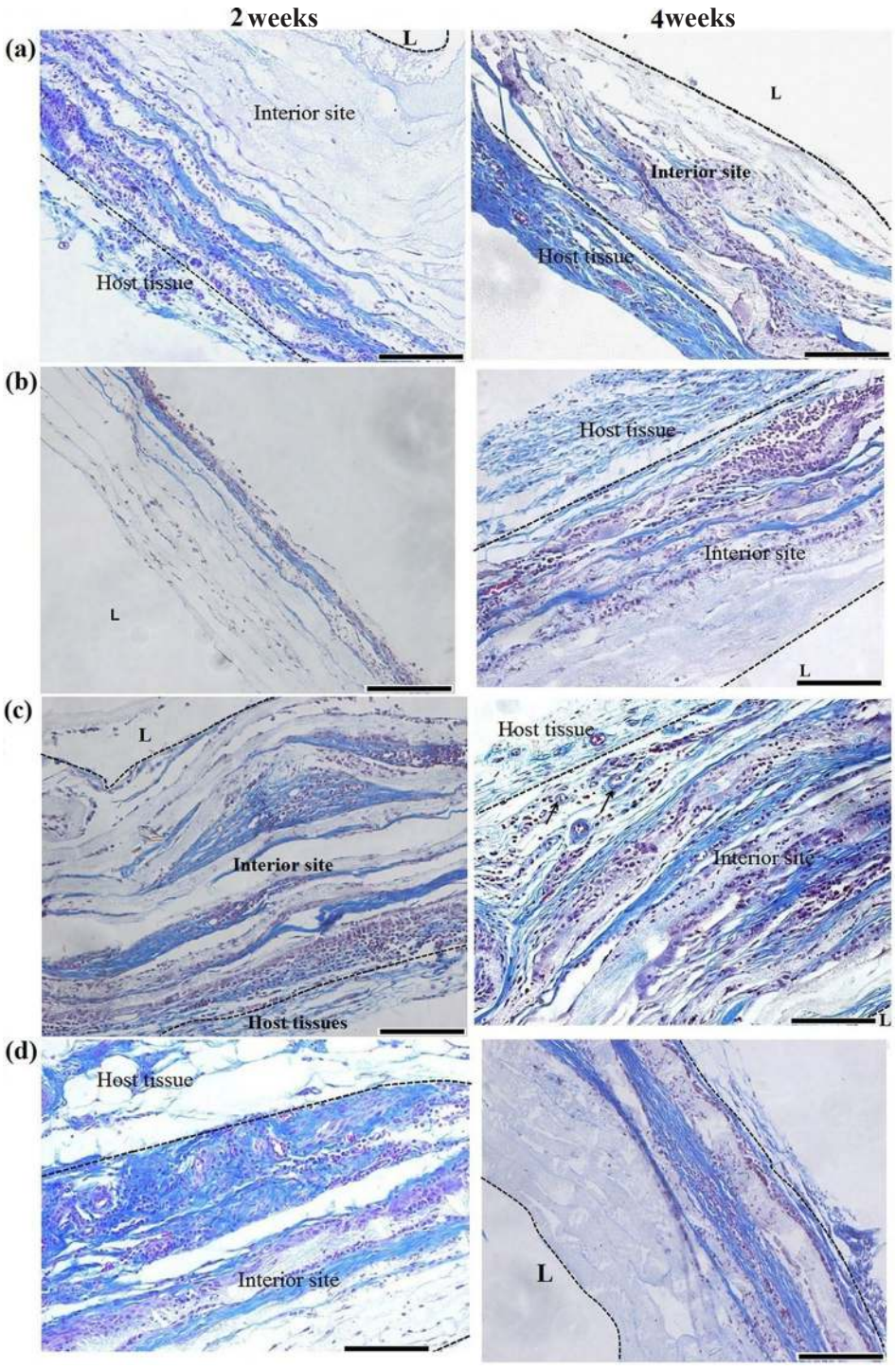

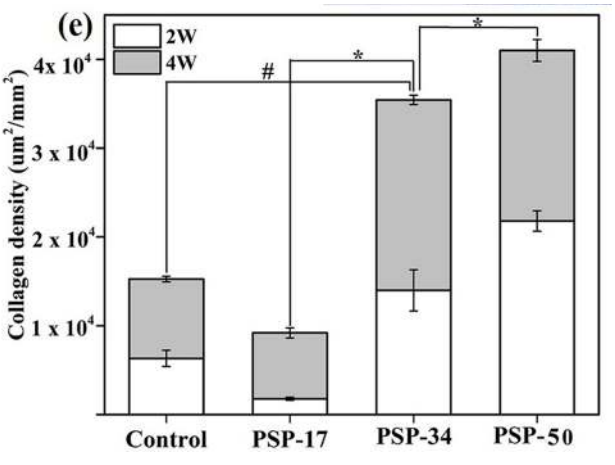

Fig. 5. Masson's trichrome staining of explanted scaffolds 2 and 4 weeks after implantation. (**a**) Control; (**b**) PSP-17 (**c**) PSP-34; and (**d**): PSP-50. Dashed lines represent the boundaries between surrounding tissues and scaffolds. Left and right panels show 2-weeks and 4-weeks groups, respectively. "L" represents lumen of samples. Scale bars, 100 μm. (**e**) Quantification of collagen ($\mu m^2/mm^2$). Masson's trichrome staining showed a higher extent of collagen deposition in PSP-34 and PSP-50 than in the control and PSP-17 group. *, # = significantly different from other groups, $^{*}p < 0.05$, $^{\#}p < 0.02$, Student's *t*-test. Data are expressed as mean ± S.D for $n = 6$.

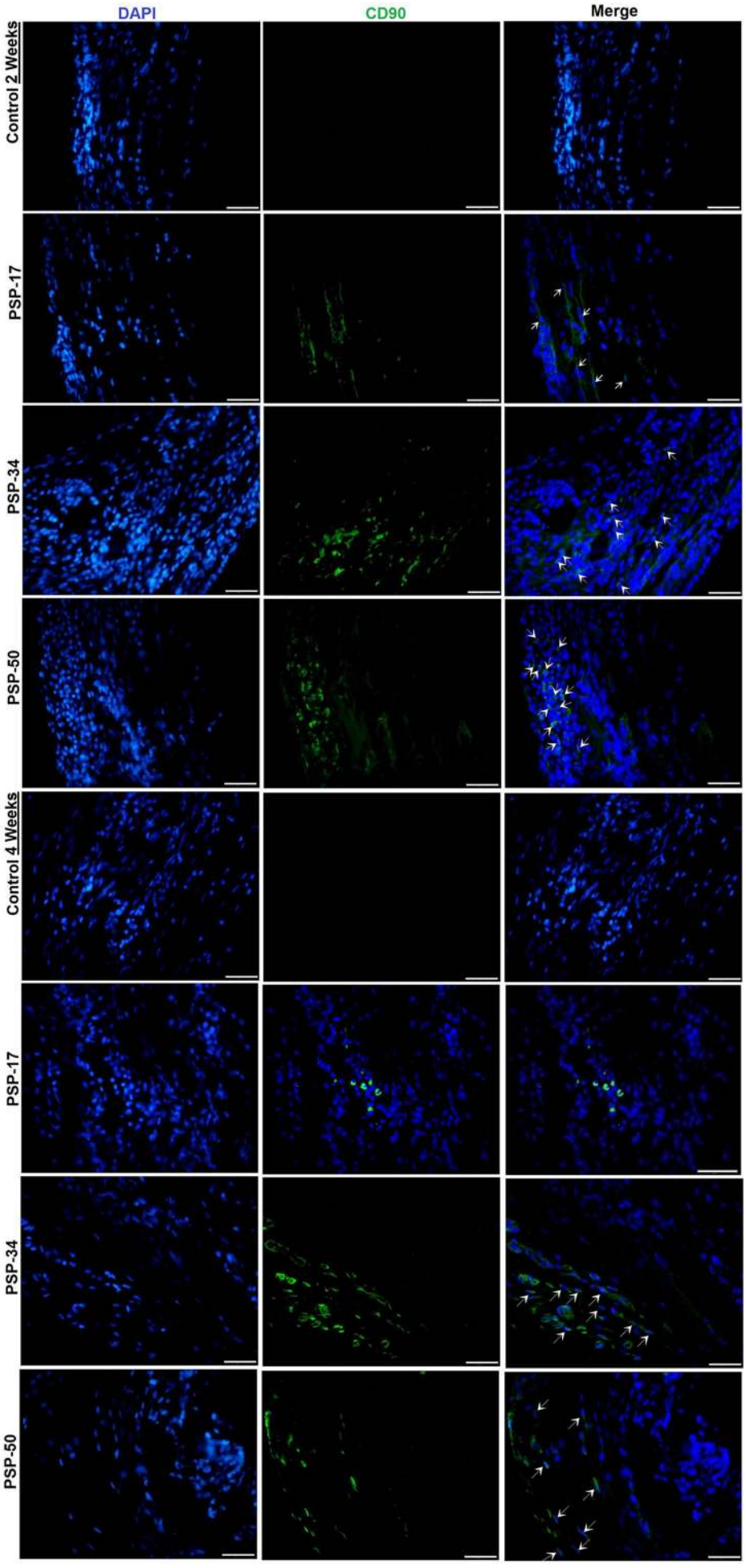

Fig. 6. *In vivo* stem cell recruitment in explanted scaffolds after 2 and 4 weeks of implantation. Sections were stained with CD90 antibody. Scaffolds containing PLCL-SP showed significantly large number of CD90 positive cells than that of the control group at both time points. Of studied groups, PSP-34 showed higher MSCs recruitment than that of the other groups ($n = 6$, $p < 0.05$). Arrows point at the $CD90^+$ cells in the scaffolds. Scale bars, 50 µm.

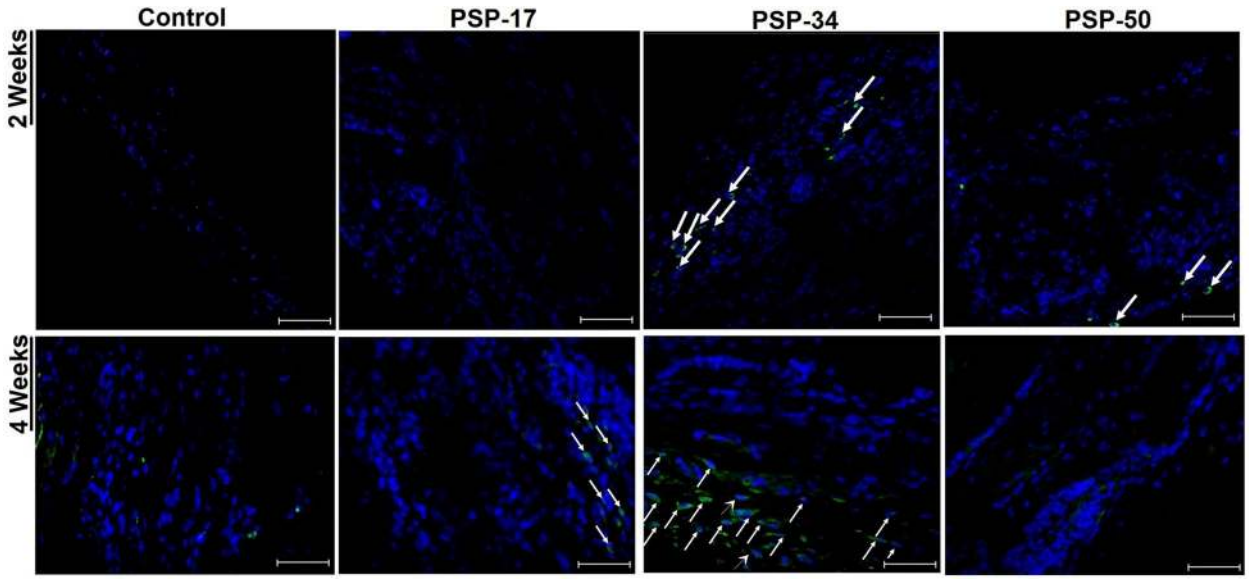

Fig. 7. *In vivo* stem cell recruitment in explanted scaffolds after 2 weeks (upper panel,) and 4 weeks (lower panel,) of implantation. Sections were stained with CD105 antibody. Control group did not show $CD105^+$ cells at both time points. Scaffolds containing PLCL-SP showed large number of CD105 positive cells ($n = 6$, $p < 0.05$). Of studied groups, PSP-34 showed higher MSCs recruitment than that of the other groups. Arrows point at $CD105^+$ cells in the scaffolds. Scale bars, 50 μm.

slightly less collagen deposition at day 28 than that at day 14. Subsequently, the levels of collagen deposited in the tissues were examined by measuring the integrated optical density of trichrome stained images. A graph quantifying these results is shown in Fig. 5e. As can be seen from the figure, PSP-17 showed less deposition of collagen than the control group did. PSP-34 and PSP-50 scaffolds showed significantly higher amounts of collagen deposition compared with the control group (Student's *t*-test, $p < 0.05$).

Effect of SP on stem cell recruitment in vivo

We further characterised the response of host stem cells to PLCL and PLCL/PLCL-SP grafts *in vivo* and evaluated whether stem cells resided in or surrounded the vascular scaffolds. We performed immunofluorescence staining of the explants with MSC-specific markers (CD90 and CD105) 14 and 28 d after implantation. Fig. 6 shows the representative micrographs of implanted grafts in the control and SP groups that have been immunostained for CD90 antibody. The control group showed only few $CD90^+$ cells at 4 weeks after implantation. On the other hand, the retrieved scaffolds in the SP group contained many $CD90^+$ cells. We also performed immunostaining for CD105 in the grafts explanted 14 and 28 d after implantation (Fig.7). The control group did not show $CD105^+$ cells while in contrast, $CD105^+$ cells were observed in the SP groups. To quantify these results, the number of $CD90^+$ and $CD105^+$ cells was counted in the merged images and shown in Fig. 8a-b. The PSP-34 group produced the highest number of $CD90^+$ and $CD105^+$ cells within the implanted scaffolds (Student's *t*-test, $p < 0.05$). The PSP-50 graft showed fewer $CD90^+$ and $CD105^+$ cells 28 d after implantation compared with the PSP-34 group. We speculate that the lower numbers of MSCs observed in this group may be due to an inhibitory or toxic effect of the higher concentration of SP. However, further studies are warranted to elucidate this.

Angiogenesis in the explanted grafts

The angiogenesis in the implanted scaffolds was evaluated by immunostaining for laminin. Fig. 9 show the confocal images of control and SP groups retrieved after 14 and 28 d that were immunostained with laminin. Very few laminin-positive blood vessels were found in the controls implanted for 14 and 28 d. However, significant growth of blood vessels occurred in the PLCL/PLCL-SP vascular scaffolds implanted for 14 and 28 d (Student's *t*-test, $n = 6$, $p < 0.05$). The numbers of laminin-positive blood vessels were counted and shown in Fig. 8c.

Evaluation of endothelial cells

The samples were stained for an endothelial cell marker, Von Willebrand factor (vWF), to further identify the types of infiltrating cells and to evaluate the extent of angiogenesis. In a comparison of the control and SP groups, the number of vWF^+ blood vessels and cells was significantly higher in the grafts containing SP at all time points (student's *t*-test, $p < 0.05$) (Fig. 10). Very few vWF^+ blood vessels were observed in the controls implanted for 14 and 28 d. The scaffolds containing SP (PSP-17) showed a larger number of vWF^+ blood vessels and cells than that in the control group. However, the interior of these grafts was free of vWF^+ vessels and cells. Of note, many vWF^+ blood vessels and cells were observed in the PSP-34 and PSP-50 groups. PSP-50 group showed fewer numbers of cells 28 d after implantation. The vWF^+ vessels (# *per*

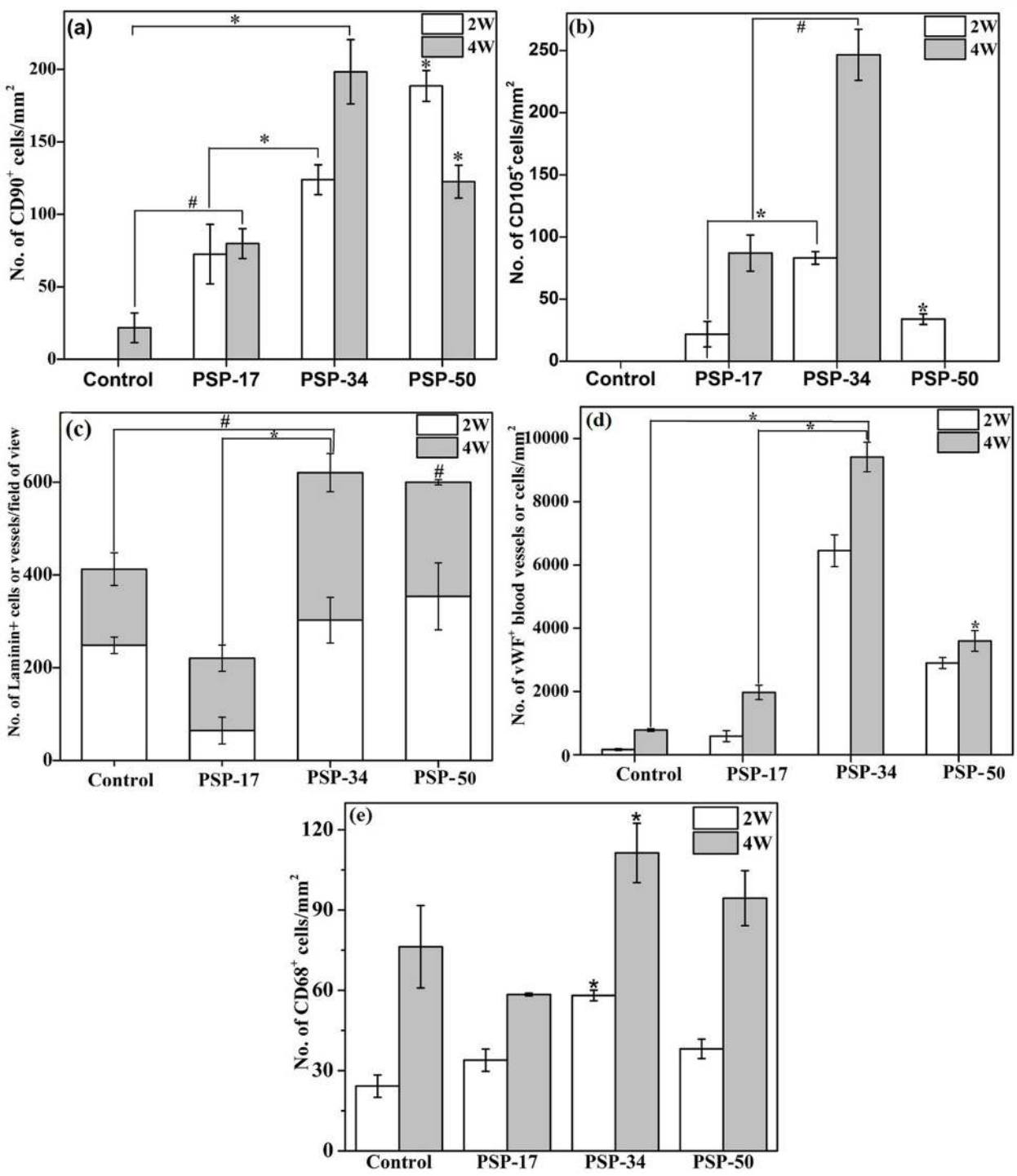

Fig. 8. Quantitative analysis of the CD90$^+$ cells, CD105$^+$ cells, laminin$^+$ blood vessels, vWF$^+$ blood vessels or cells, and CD68$^+$ macrophages in PLCL and PLCL/PLCL-SP scaffolds after 2 weeks (2W) and 4 weeks (4W) of implantation. (**a**) No. of CD90$^+$ cells. (**b**) No. of CD105$^+$ cells. PLCL-SP containing scaffolds showed significantly higher numbers of CD90$^+$ and CD105$^+$ cells 2 and 4 weeks after implantation compared with control groups. Of studied groups, PSP-34 scaffolds showed higher numbers of MSCs. (**c**) No. of laminin positive blood vessels *per* field of view. (**d**) No. of vWF$^+$ blood vessels *per* mm^2. PSP-34 showed significantly higher numbers of laminin$^+$ and vWF$^+$ blood vessels or cells than that of the control group at both time points. PSP-50 showed less numbers of vWF$^+$ cells than that of PSP-34 group. (**e**) No. of CD 68$^+$ cells *per* mm^2 in the retrieved scaffolds 2 and 4 weeks after implantation. Only few macrophages were observed in the scaffolds explanted after 2 weeks. Scaffolds explanted after 4 weeks show higher extent of CD 68$^+$ cells. *, # = significantly different from other groups, *$p < 0.05$, $^{\#}p < 0.02$, Student's *t*-test. Data are expressed as mean ± SD for $n = 8$.

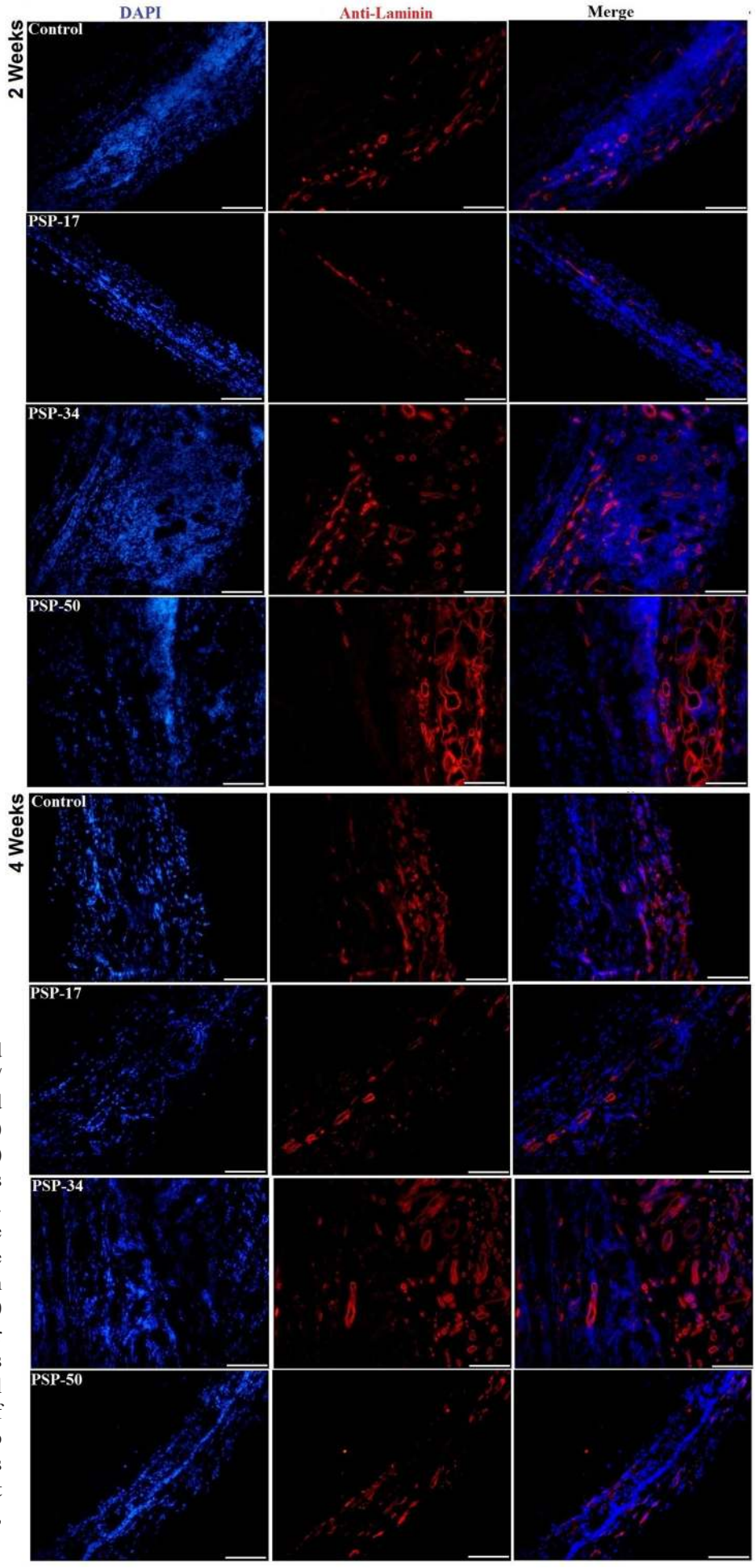

Fig. 9. Evaluation of blood vessels in PLCL and PLCL/PLCL-SP scaffolds retrieved after 2 weeks (left panel) and 4 weeks (right panel) of implantation. Samples were stained with laminin. Blood vessels were seen at the tissue/scaffold interface in the control and PSP-17 groups. In contrast, PSP-34 and PSP-50 grafts showed large number of laminin^{+} blood vessels compared with the control group (n = 6, $p < 0.05$). Of studied groups, PSP-34 group showed the highest numbers of blood vessels formation at both time points. Scale bars, 100 μm.

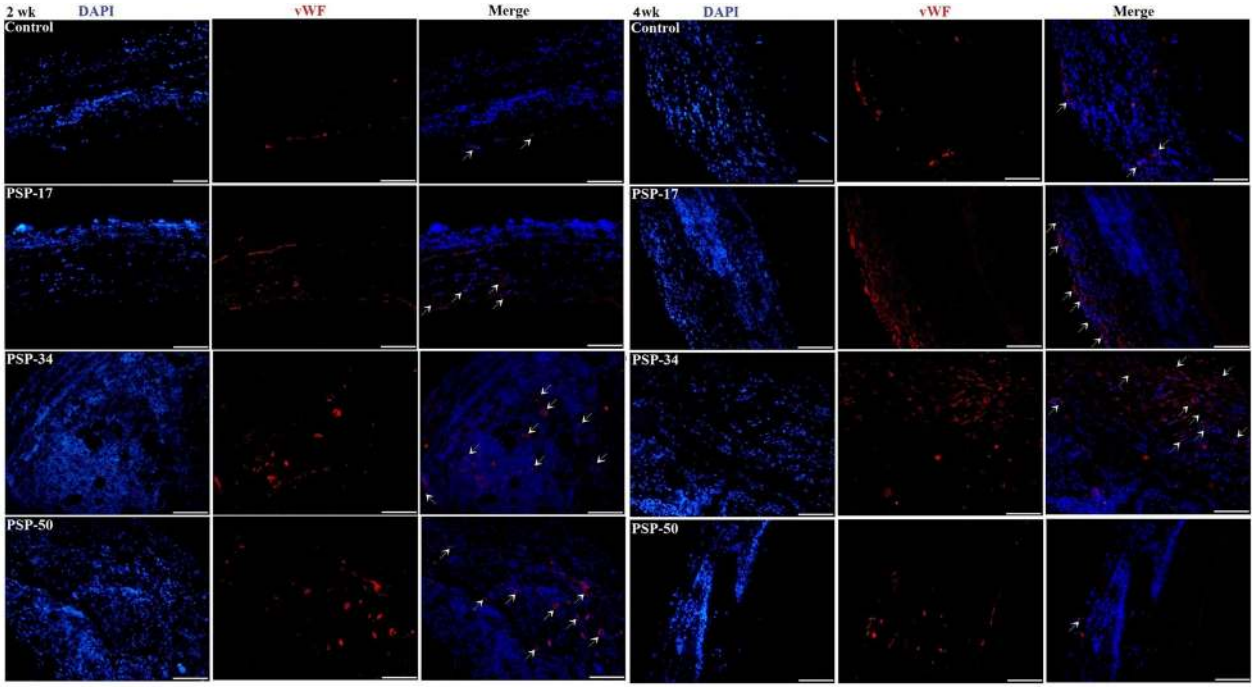

Fig. 10. Evaluation of vWF^+ blood vessels and cells in PLCL and PLCL/PLCL-SP scaffolds after 2 weeks (left panel) and 4 weeks (right panel) of implantation. Control and PSP-17 grafts showed less numbers of vWF^+ blood vessels 2 and 4 weeks after implantation. PSP-34 and PSP-50 groups showed large numbers of vWF^+ blood vessels and cells compared with the control group. Of studied groups, PSP-34 group showed the highest numbers of blood vessels or cells at both time points. Arrows point at vWF^+ blood vessels or cells in the scaffolds. Scale bars, 100 μm.

mm^2) in each group were quantified using Image J ($n = 4$ in each group; Fig. 8d).

Evaluation of inflammatory macrophages

We also performed immunostaining of explanted scaffolds with the pan macrophage marker "CD68" to evaluate the inflammatory response and the confocal micrographs obtained are shown in Fig. 11. Both PLCL and PLCL/PLCL-SP scaffolds showed only few $CD68^+$ cells 14 d after implantation. The number of $CD68^+$ cells was higher 28 d after implantation. We also quantified the number of $CD68^+$ cells and the results are shown in Fig. 8e.

Discussion

Recently, *in situ* TE approaches for artificial blood vessels have been reported, and these systems were shown to induce vascular regeneration through endogenous cell recruitment. In addition to various chemotactic agents such as G-CSF, GM-CSF, and SDF-1α, SP has been suggested as a new potential bioactive molecule that can accelerate tissue regeneration through endogenous cell mobilisation and immune-modulatory mechanisms (Hong *et al*., 2009; Amadesi *et al*., 2012; Kim *et al*., 2015). Substance P exerts its effects by preferentially binding to and activating the tachykinin receptor neurokinin 1 (NK1) receptor (Amadesi *et al*., 2012). In previous studies, SP has either been encapsulated in hydrogels or immobilised on pre-fabricated sponges and scaffolds. However, these approaches only minimally allow for large-scale processing manipulation. Therefore, we emphasise the conjugation of SP with PLCL in bulk to achieve effective delivery for an extended period and the fabrication of ES scaffolds as artificial vascular grafts from this modified copolymer. PLCL-SP provides local delivery of SP in scaffolds, which can induce tissue regeneration *via* the local and systematic cellular and immune-modulatory effects of SP. We fabricated PLCL/PLCL-SP scaffolds containing different doses of SP to provide a series of scaffolds.

Nanofibres were found to be smooth and homogeneous. The fibrous structure stimulates the microstructure of native arteries and allows the integration of the scaffold with the surrounding cells and native arteries. The average diameter of the fibres increased in the following order: PSP-50 < PSP-34 < PSP-17 < control. This might be due the addition of low molecular weight PLCL-SP copolymer. Our results also indicate that SP was released in a sustained fashion and the released amount of SP was comparable in the three groups. *In vitro*, SP might be released from the meshes as a result of hydrolysis. During *in vivo* implantation, PLCL is degraded hydrolytically and enzymatically (Jeong *et al*., 2004). These results indicate that the meshes containing covalently conjugated SP can provide long-term persistence of this biomolecule *in vivo*, which can be very effective for cell recruitment, proliferation, and/or differentiation. Because SP has a very short half-life *in vitro* and is rapidly degraded by enzymes, it is imperative to design suitable biomaterials that can preserve its bioactivity and enhance its *in vivo* stability (Hong *et al*., 2009). In previous reports from our group, we found that long-term and localised persistence

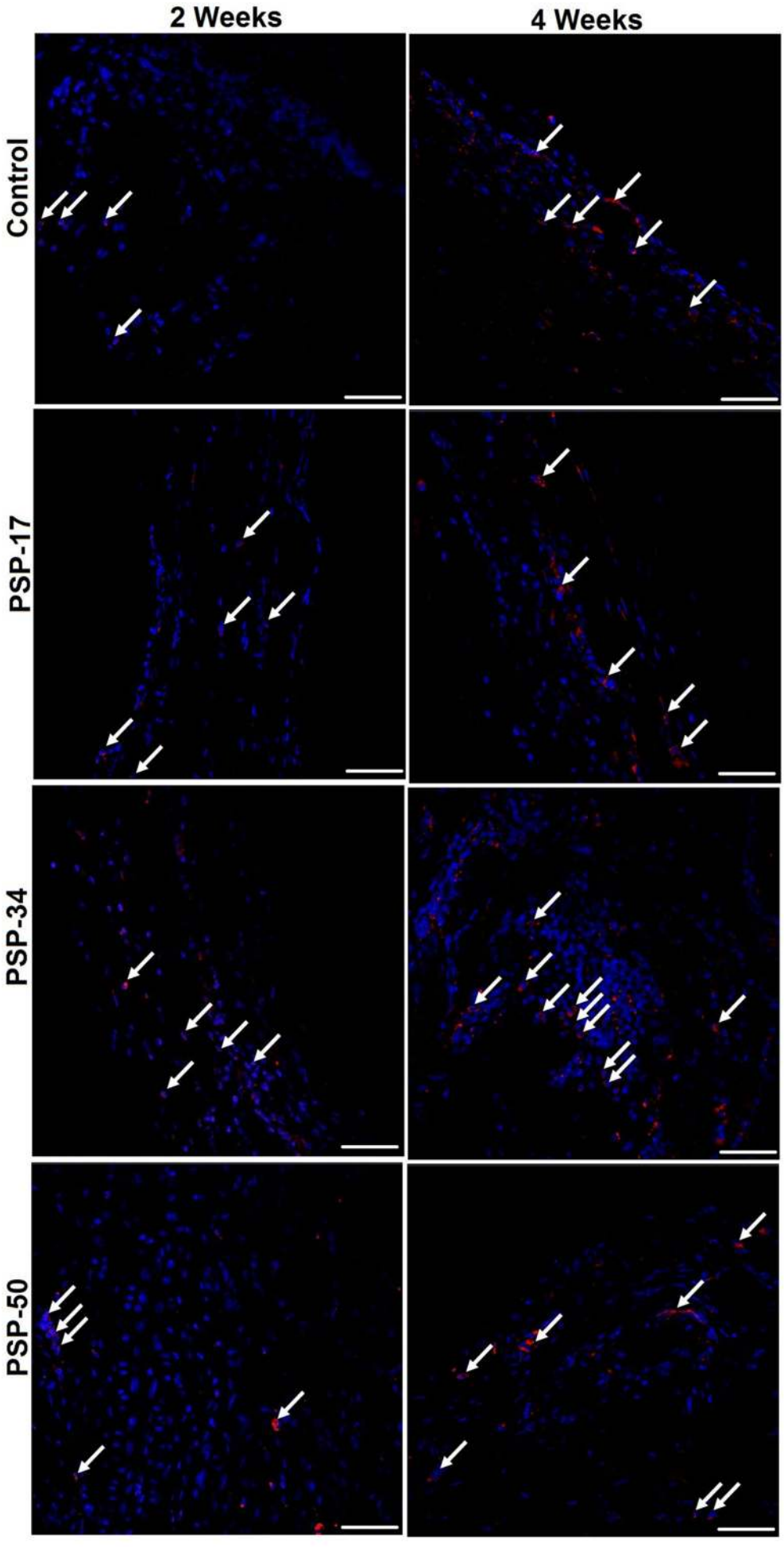

Fig. 11. Evaluation of $CD68^+$ macrophages in PLCL and PLCL/PLCL-SP scaffolds after 2 weeks (upper panel) and 4 weeks (lower panel) of implantation. Arrows point at the $CD68^+$ cells. Scaffolds explanted at 4 weeks showed more macrophages than at 2 weeks. Scale bars, 50 μm.

of SP in self-assembling peptides enhanced ischemic revascularisation and bone regeneration (Kim *et al*., 2013; Kim *et al*., 2015). This study has demonstrated that the bioactivity of SP was preserved and scaffolds containing SP significantly induced the migration of hMSCs *in vitro* compared with the negative control (Fig. 3). Quantitative analysis showed that the extent of hMSC recruitment was dependent on SP content in different meshes. Our results are consistent with those from previous studies (Hong *et al*., 2009; Amadesi *et al*., 2012; Kim *et al*., 2015).

Cell infiltration is the initial step with a critical role in the subsequent regeneration of vascular grafts through processes such as vascularisation, ECM secretion, and deposition (Zilla *et al*., 2007). Limited cell infiltration often prevents the long-term regeneration and remodelling process of vascular grafts (de Valence *et al*., 2012). To address this issue, two strategies have been adopted to date. One is to focus on rapid degradation, whereas the second is to increase the pore size of the scaffolds. The space generated during degradation promotes cell infiltration and tissue regeneration (Wu *et al*., 2012). Since PLCL (50:50) is a biodegradable copolymer, it will be degraded and sorbed after implantation. Consequently, host cells can infiltrate into the grafts and induce vascular regeneration. Our data demonstrated that cells only slightly infiltrated into the control and PSP-17 grafts. Of these grafts, PSP-17 showed lower cell infiltration 14 d after implantation, which might be due to smaller diameter of nanofibres (Fig. 4b). It has been documented that cellular infiltration into ES scaffolds is often impeded by the high packing density of the fibres (Balguid *et al.,* 2009). The experimental evidence indicated a significant enhancement of cell infiltration in the PSP-34 and PSP-50 grafts. Homogeneous cell distribution was achieved in these groups 14 d after implantation. While SP-containing groups possess almost similar morphology, the higher cell population of PSP-34 and PSP-50 grafts might be attributed to the role of SP in enhancing host cell recruitment, proliferation, and/or differentiation (Kohara *et al.,* 2010; Kim *et al*., 2014; La *et al*., 2014; Hong *et al*., 2015). Since our system enables the localised presence of SP in the scaffold, we expect that it might have produced a favourable microenvironment for host cell infiltration as well as for their proliferation and differentiation, thus enhancing reparative effects (Jin *et al.,* 2015). We speculate that several types of cells such as fibroblasts, myofibroblasts, macrophages, vascular cells, and stem cells, can infiltrate into the scaffolds. These cells may be mobilised from resident tissues, circulation, or BM. Indeed, our results indicate the presence of ECs, MSCs, and few $CD68^+$ macrophages.

Deposition, remodelling, and organisation of the ECM by fibroblasts are essential functions for tissue growth. Histological trichrome staining performed to identify the presence of collagen in the scaffolds showed more collagen deposition in the PSP-34 and PSP-50 groups than in the controls and PSP-17. These results suggest that infiltrated cells were functional and secreted ECM. Indeed, SP is assumed to enhance the healing process partly by stimulating the proliferation of fibroblasts, myofibroblasts, and notably stem/progenitor cells, in turn leading to enhanced collagen formation and organisation (Nilsson *et al*., 1985; Carlsson *et al*., 2011; Hong *et al*., 2009). PSP-17 scaffolds showed slightly lower collagen deposition than the controls did 14 d after implantation, which was attributed to the accumulation of only few cells and less cell proliferation (Fig. 5b). Immune-modulatory response was assessed by pan-macrophage staining in the scaffolds. Although significant differences between the numbers of macrophages in the control and SP groups were not observed 14 d after implantation, slightly more macrophages were observed in PSP-34 than in the controls implanted for 28 d. Further identification of macrophage phenotypes is needed to define the dominant activity of infiltrating macrophages.

Previous studies have documented that the SP gradient between circulation and BM resulted in the recruitment of $NK1^+$ stem/progenitor cells towards damaged tissues, and that these cells promoted ischemic revascularisation and tissue regeneration (Hong *et al*., 2009; Amadesi *et al*., 2012; Kim *et al*., 2014; Noh *et al*., 2015). This study confirmed that the scaffolds containing SP recruited MSCs *in vivo* and that these scaffolds were more effective in MSC recruitment than the control groups were at all observed time points. PSP-34 grafts showed a higher number of MSCs 14 and 28 d after implantation. Unexpectedly, fewer numbers of cells were observed in PSP-50 28 d after implantation, which may be due to an inhibitory or toxic effect of the higher concentration of SP by this time point. However, further studies are warranted to confirm this speculation. Potentially, such cell recruitment could be augmented or differentiated into various lineages by providing suitable signalling molecules (Amadesi *et al*., 2012; Hong *et al*., 2015). Given that SP induces the differentiation of stem cells into multiple lineages, the localised presence of SP within the vascular scaffolds could endow a suitable microenvironment for vascular regeneration (Fu *et al*., 2014; Noh *et al*., 2015). Though the exact origin of the recruited cells is not yet known, these cells might have been recruited from the BM, circulation, or adipose tissues (Hong *et al*., 2009; Ko *et al*., 2012; Mun *et al*., 2013).

Scaffold vascularisation was examined by immunostaining explanted scaffolds for laminin and Von Willebrand factor (vWF) that is a mandatory prerequisite for functional tissues. After implantation, all infiltrating cells depend on adequate supplies of oxygen and nutrients for survival. Therefore, it is critical for scaffold to develop sufficient vasculature. The control and PSP-17 groups showed blood vessel ingrowth mainly at the tissue-scaffold interface, whereas the PSP-34 scaffold showed evidence for angiogenesis throughout the cross-section. PSP-50 showed less vascularisation 28 d after implantation than observed after 14 d, which may be due to an inhibitory or toxic effect of SP (Fig. 8c). Further studies are needed confirm this. Thus, the incorporation of PLCL-SP in the scaffolds could enhance angiogenesis possibly through the enhanced recruitment of MSC, which gives rise to therapeutic potential in TE. We speculate that the beneficial effects of scaffolds containing SP are as a result of (1) their MSC-recruiting ability with angiogenic capability, and (2) the long-term release of SP. It has been reported that SP not only recruits MSC, but also various angiogenic cells

in vitro and *in vivo* that have been shown to participate in angiogenesis (Ziche *et al*., 1990; Hong *et al*., 2009; Kohara *et al*., 2010; Kim *et al.*, 2013). Overall it is possible that recruited stem cells, progenitor cells, or vascular cells proliferated and sometimes differentiated, inducing angiogenesis (Kim *et al.*, 2014). These neo-vessels might have formed from the recruitment of ECs and SMCs from adjacent vessel segments. Furthermore, host-derived cells may participate in the formation of neo-vessel through a paracrine mechanism by initiating an immune-modulatory cytokine cascade necessary for vascular neotissues formation, including the proliferation and migration of ECs and SMCs in addition to ECM production and tissue regeneration.

In summary, we have demonstrated that TEVGs incorporated with PLCL-SP have the ability to grow, repair, and remodel. While this study demonstrated the potential of SP in enhancing tissue regeneration in ES scaffolds, the strategy can be extended to other biomaterial scaffolds for applications such as cartilage TE, bone TE, and wound healing. Future developments of this method may allow SP as well as other peptides or growth factors to be conjugated with other synthetic or natural polymeric materials. Different combinations of regulatory signals, including growth factors, cell adhesion molecules, or a balanced combination of the two, can be conjugated with the activated functional groups of the star-shaped PLCL to simultaneously enhance stem cell mobilisation, homing, and angiogenesis. These materials can be fabricated into different shapes and structures such as, membranes, spheres, and scaffolds as needed for the TE of additional organs and tissues to improve tissue repair. The SP-conjugated polymers can be directly electrospun or printed (using 3D printing) to yield off-the-shelf small-diameter vascular grafts. Thus, the current study provides a promising solution for the sustained signalling of neuropeptides in ES meshes to promote stem cell recruitment, which might be critical for *in situ* tissue regeneration.

Our study has limitations in that we evaluated the performance of the 3D scaffolds after subcutaneous implantation. When implanted as a vascular substitute, the grafts would be in an environment that is completely different from that after simple subcutaneous implantation. Therefore, the characterisation of these grafts as vascular substitutes will further delineate the potential of this strategy. Therefore, this study warrants the assessment of these TEVGs as vascular interposition grafts in flow conditions. In particular, a careful elucidation of stenosis, aneurismal dilation, rupture, and thrombosis will clarify the potential of our strategy in the development of TEVGs. Recently, it has been shown that macrophages and their phenotypes are essential for tissue regeneration, neovascularisation, and graft complications such as stenosis. Detailed characterisations of macrophages and their phenotypes may be another direction of this study.

Conclusion

In the current study, we have developed electrospun scaffolds containing different concentrations of SP (16.4, 33.3, and 49.7 nmol/g of the mesh) to fabricate vascular grafts, and evaluated their performance *in vitro* and *in vivo*. ELISA revealed the sustained release of SP and *in vitro* cell migration assay showed the recruitment of hMSCs towards SP containing electrospun mats. The 3D scaffolds containing SP showed significantly higher host cell infiltration, blood vessel formation, and MSC recruitment *in vivo* compared with the control group. Of the investigated groups, PSP-34 showed higher cell infiltration, MSC recruitment, and blood vessel formation. The strategy adopted here could be employed to functionalise polymeric biomaterials to induce stem cell recruitment and promote blood vessel formation.

Acknowledgments

This work was supported by the Ministry of Trade, Industry and Energy, Republic of Korea (Project Number 10052732).

Disclosure Statement

The authors do not have conflict of interest.

References

Amadesi S, Reni S, Katare R, Meloni M, Oikawa A, Beltrami AP, Avolio E, Cesselli D, Fortunato O, Spinetti G, Ascione R, Cangiano E, Valgimigli M, Hunt SP, Emanueli C, Madeddu P (2012) Role for substance p-based nociceptive signals in progenitor cell activation and angiogenesis during ischemia in mice and human subjects. Circulation **125**: 1774-1786.

Askari AT, Unzek S, Popovic ZB, Goldman CK, Forudi F, Kiedrowski M, Rovner A, Ellis SG, Thomas JD, DiCorleto PE, Topol EJ, Penn MS (2003) Effect of stromal-cell-derived factor 1 on stem-cell homing and tissue regeneration in ischaemic cardiomyopathy. Lancet **362**: 697-703.

Balguid A, Mol A, van Marion MH, Bank RA, Bouten CV, Baaijens FP (2009) Tailoring fiber diameter in electrospun poly(epsilon-caprolactone) scaffolds for optimal cellular infiltration in cardiovascular tissue engineering. Tissue Eng Part A **15**: 437-444.

Carlsson O, Schizas N, Li J, Ackermann PW (2011) Substance P injections enhance tissue proliferation and regulate sensory nerve ingrowth in rat tendon repair. Scand J Med Sci Sports **21**: 562-569.

Chen FM, Wu LA, Zhang M, Zhang R, Sun HH (2011) Homing of endogenous stem/progenitor cells for *in situ* tissue regeneration: Promises, strategies, and translational perspectives. Biomaterials **32**: 3189-3209.

Cho SW, Lim JE, Chu HS, Hyun HJ, Choi CY, Hwang KC, Yoo KJ, Kim DI, Kim BS (2006) Enhancement of *in vivo* endothelialization of tissue-engineered vascular grafts by granulocyte colony-stimulating factor. J Biomed Mater Res A **76**: 252-263.

Choi JS, Leong KW, Yoo HS (2008) *In vivo* wound healing of diabetic ulcers using electrospun nanofibers

immobilized with human epidermal growth factor (EGF). Biomaterials **29**: 587-596.

Chun C, Lim HJ, Hong KY, Park KH, Song SC (2009) The use of injectable, thermosensitive poly (organophosphazene)-RGD conjugates for the enhancement of mesenchymal stem cell osteogenic differentiation. Biomaterials **30**: 6295-6308.

Cook AD, Hrkach JS, Gao NN, Johnson IM, Pajvani UB, Cannizzaro SM (1997) Characterization and development of RGD-peptide-modified poly (lactic acid-co-lysine) as an interactive, resorbable biomaterial. J Biomed Mater Res **35**: 513-523.

de Valence S, Tille JC, Mugnai D, Mrowczynski W, Gurny R, Möller M, Walpoth BH (2012) Long term performance of polycaprolactone vascular grafts in a rat abdominal aorta replacement model. Biomaterials **33**: 38-47.

De Visscher G, Mesure L, Meuris B, Ivanova A, Flameng W (2012) Improved endothelialization and reduced thrombosis by coating a synthetic vascular graft with fibronectin and stem cell homing factor SDF-1α. Acta Biomater **8**: 1330-1338.

Epstein AJ, Polsky D, Yang F, Yang L, Groeneveld PW (2011) Coronary revascularization trends in the United States: 2001-2008. JAMA **305**: 1769-1776.

Fu S, Mei G, Wang Z, Zou ZL, Liu S, Pei GX, Bi L, Jin D (2014) Neuropeptide substance P improves osteoblastic and angiogenic differentiation capacity of bone marrow stem cells *in vitro*. Biomed Res Int: Article ID 596023.

Gimble JM, Katz AJ, Bunnell BA (2007) Adipose-derived stem cells for regenerative medicine. Circ Res **100**: 1249-1260.

Go DH, Joung YK, Park SY, Park YD, Park KD (2008) Heparin-conjugated star-shaped PLA for improved biocompatibility. J Biomed Mater Res Part A **86**: 842-848.

Hashi CK, Zhu Y, Yang GY, Young WL, Hsiao BS, Wang K, Chu B, Li S (2007) Antithrombogenic property of bone marrow mesenchymal stem cells in nanofibrous vascular grafts. Proc Natl Acad Sci USA **104**: 11915-11920.

Hassan K, Kim SH, Park I, Lee SH, Kim SH, Jung Y, Kim S-H, Kim SH (2011). Small diameter double layer tubular scaffolds using highly elastic PLCL copolymer for vascular tissue engineering. Macromol Res **19**: 122-129.

Heissig B, Hattori K, Dias S, Friedrich M, Ferris B, Hackett NR, Crystal RG, Besmer P, Lyden D, Moore MA, Werb Z, Rafii S (2002) Recruitment of stem and progenitor cells from the bone marrow niche requires MMP-9 mediated release of kit-ligand. Cell **109**: 625-637.

Hibino N, Villalona G, Pietris N, Duncan DR, Schoffner A, Roh JD, Yi T, Dobrucki LW, Mejias D, Sawh-Martinez R, Harrington JK, Sinusas A, Krause DS, Kyriakides T, Saltzman WM, Pober JS, Shin'oka T, Breuer CK (2011) Tissue-engineered vascular grafts form neovessels that arise from the regeneration of adjacent vessels. FASEB J **25**: 2731-2739.

Hoerstrup SP, Cummings MI, Lachat M, Schoen FJ, Jenni R, Leschka S, Neuenschwander S, Schmidt D, Mol A, Günter C, Gössi M, Genoni M, Zund G (2006) Functional growth in tissue-engineered living, vascular grafts: follow-up at 100 weeks in a large animal model. Circulation **114 (1 Supp)**: I159-I166.

Hiramoto M, Aizawa S, Iwase O, Nakano M, Toyama K, Hoque M, Nabeshima R, Kaidow A, Imai T, Hoshi H, Handa H (1998). Stimulatory effects of Substance P on CD34 positive cell proliferation and differentiation *in vitro* are mediated by the modulation of stromal cell function. Int J Mol Med **1**: 347-354.

Hong HS, Lee J, Lee E, Kwon YS, Lee E, Ahn W, Jiang MH (2009) A new role of substance P as an injury-inducible messenger for mobilization of CD29(+) stromal-like cells. Nat Med **15**: 425-435.

Hong HS, Kim do Y, Yoon KJ, Son Y (2011) A new paradigm for stem cell therapy: substance-P as a stem cell-stimulating agent. Arch Pharm Res **34**: 2003-2006.

Hong HS, Son Y (2014) Substance-p-mobilized mesenchymal stem cells accelerate skin wound healing. Tissue Eng Regen Med **11:** 483-491.

Hong HS, Kim S, Nam S, Um J, Kim YH, Son, Y (2015) Effect of substance P on recovery from laser-induced retinal degeneration. Wound Repair Regen **23**: 268-277.

Jeong SI, Kim BS, Lee YM, Ihn KJ, Kim SH, Kim YH (2004) Morphology of elastic poly (L-lactide-co-epsilon- caprolactone) copolymers and *in vitro* and *in vivo* degradation behavior of their scaffolds. Biomacromolecules **5**: 1303-1309.

Jin Y, Hong HS, Son Y (2015) Substance P enhances mesenchymal stem cells-mediated immune modulation. Cytokine **71**: 145-153.

Karp JM, Leng Teo GS (2009) Mesenchymal stem cell homing: the devil is in the details. Cell Stem Cell **4**: 206-216.

Karapetyan AV, Klyachkin YM, Selim S, Sunkara M, Ziada KM, Cohen DA, Zuba-Surma EK, Ratajczak J, Smyth SS, Ratajczak MZ, Morris AJ, Abdel-Latif A (2013) Bioactive lipids and cationic antimicrobial peptides as new potential regulators for trafficking of bone marrow-derived stem cells in patients with acute myocardial infarction. Stem Cells Dev **22**: 1645-1656.

Kim JH, Jung Y, Kim BS, Kim SH (2013) Stem cell recruitment and angiogenesis of neuropeptide substance P coupled with self-assembling peptide nanofiber in a mouse hind limb ischemia model. Biomaterials **34**:1657-1668.

Kim TG, Park TG (2006) Surface functionalized electrospun biodegradable nanofibers for immobilization of bioactive molecules. Biotechnol Prog **22**: 1108-1113.

Kim SH, Hur W, Kim JE, Min HJ, Kim S, Min HS, Kim BK, Kim SH, Choi TH, Jung Y (2015) Self-assembling peptide nanofibers coupled with neuropeptide substance P for bone tissue engineering. Tissue Eng Part A **21**: 1237-1246.

Kim MS, Park SJ, Gu BK, Kang CM, Kim CH (2014) Substance P-immobilized Chitosan Nanofibers. Mol Cryst Liq Cryst **603**: 146-156.

Ko IK, Ju YM, Chen T, Atala A, Yoo JJ, Lee SJ (2012) Combined systemic and local delivery of stem cell inducing/recruiting factors for *in situ* tissue regeneration. FASEB J **26**: 158-168.

Kohara H, Tajima S, Yamamoto M, Tabata Y (2010) Angiogenesis induced by controlled release of neuropeptide substance P. Biomaterials **31**: 8617-8625.

Kuhl PP, Griffith-Cima LG (1996) Tethered epidermal growth factor as a paradigm for growth factor-induced stimulation from the solid phase. Nat Med **2**: 1022-1027.

La WG, Jin M, Park S, Yoon HH, Jeong GJ, Bhang SH, Park H, Char K, Kim BS (2014) Delivery of bone morphogenetic protein-2 and substance P using graphene oxide for bone regeneration. Int J Nanomedicine **9 (Suppl 1)**: 107-116.

Lee CH, Cook JL, Mendelson A, Moioli EK, Yao H, Mao JJ (2010) Regeneration of the articular surface of the rabbit synovial joint by cell homing: a proof of concept study. Lancet **376**: 440-448.

Lee J, Yoo JJ, Atala A, Lee SJ (2012) The effect of controlled release of PDGF-BB from heparin-conjugated electrospun PCL/gelatin scaffolds on cellular bioactivity and infiltration. Biomaterials **33**: 6709-6720.

Lee K-W, Johnson NR, Gao J, Wang Y (2013) Human progenitor cell recruitment *via* SDF-1α coacervate laden PGS vascular grafts. Biomaterials **34**: 9877-9885.

Lee SJ, Van Dyke M, Atala A, Yoo JJ (2008) Host cell mobilization for *in situ* tissue regeneration. Rejuvenation Res **11**: 747-756.

L'Heureux N, Paquet S, Labbe R, Germain L, Auger FA (1998) A completely biological tissue-engineered human blood vessel. FASEB J **12**: 47-56.

Lotz M, Carson DA, Vaughan JH (1987) Substance P activation of rheumatoid synoviocytes: neural pathway in pathogenesis of arthritis. Science **235**: 893-895.

Momin F, Kraut M, Lattin P, Valdivieso M (1992) Thrombocytopenia in patients receiving chemoradiotherapy and G-CSF for locally advanced non-small cell lung cancer (NSCLC). In Proc Am Soc Clin Oncol **11**, 1632.

Mun CH, Kim SH, Jung Y, Kim SH, Kim AK, Kim DI, Kim SH (2013) Elastic, double-layered poly (l-lactide-co-ε-caprolactone) scaffold for long-term vascular reconstruction. J Bioact Compat Polym **28**: 233-246.

Mun CH, Jung Y, Kim SH, Lee SH, Kim HC, Kwon IK, Kim SH (2012) Three-dimensional electrospun poly(lactide-co-ε-caprolactone) for small-diameter vascular grafts. Tissue Eng Part A **18**: 1608-1616.

Nair A, Shen J, Lotfi P, Ko CY, Zhang CC, Tang L (2011) Biomaterials implants mediate autologus stem cell recruitment in mice. Acta Biomater **7**: 3887-3895.

Nilsson J, von Euler AM, Dalsgaard CJ (1985) Stimulation of connective tissue cell growth by substance P and substance K. Nature **315**: 61-63.

Noh SS, Bhang SH, La WG, Lee S, Shin JY, Ma YJ, Jang HK, Kang S, Jin M, Park J, Kim BS (2015) A dual delivery of substance P and bone morphogenetic protein-2 for mesenchymal stem cell recruitment and bone regeneration. Tissue Eng Part A **21**: 1275-1287.

Pektok E, Nottelet B, Tille JC, Gurny R, Kalangos A, Moeller M, Walpoth BH (2008) Degradation and healing characteristics of small-diameter poly(epsilon-caprolactone)vascular grafts in the rat systemic arterial circulation. Circulation **118**: 2563-2670.

Phadke A, Hwang Y, Kim SH, Kim SH, Yamaguchi T, Masuda K, Varghese S (2013) Effect of scaffold microarchitecture on osteogenic differentiation of human mesenchymal stem cells. Eur Cell Mater **25**: 114-129.

Pittenger MF, Mackay AM, Beck SC, Jaiswal RK, Douglas R, Mosca JD, Moorman MA, Simonetti DW, Craig S, Marshak DR (1999) Multilineage potential of adult human mesenchymal stem cells. Science **284**: 143-147.

Place ES, Evans ND, Stevens MM (2009) Complexity in biomaterials for tissue engineering. Nat Mater **8:** 457-470.

Hong JD, Sawh-Martinez R, Brennan MP, Jay SM, Devine L, Rao DA, Yi T, Mirensky TL, Nalbandian A, Udelsman B, Hibino N, Shinoka T, Saltzman WM, Snyder E, Kyriakides TR, Pober JS, Breuer CK (2010) Tissue-engineered vascular grafts transform into mature blood vessels *via* an inflammation-mediated process of vascular remodeling. Proc Natl Acad Sci USA **107**: 4669-4674.

Schantz JT, Chim H, Whiteman M (2007) Cell guidance in tissue engineering: SDF-1 mediates site-directed homing of mesenchymal stem cells within three-dimensional polycaprolactone scaffolds. Tissue Eng **13**: 2615-2624.

Shafiq M, Lee SH, Jung Y, Kim SH (2015a) Strategies for recruitment of stem cells to treat myocardial infarction. Curr Pharm Des **21**: 1584-1597.

Shafiq M, Jung Y, Kim SH (2015b) Stem cell recruitment, angiogenesis, and tissue regeneration in substance P-conjugated poly(l-lactide-co-ε-caprolactone) nonwoven meshes. J Biomed Mater Res A **103**: 2673-2688.

Shao Z, Zhang X, Pi Y, Wang X, Jia Z, Zhu J, Dai L, Chen W, Yin L, Chen H, Zhou C, Ao Y (2012) Polycaprolactone electrospun mesh conjugated with an MSC affinity peptide for MSC homing *in vivo*. Biomaterials **31**: 3375-3387.

Wu W, Allen RA, Wang Y (2012) Fast degrading elastomer enables rapid remodeling of a cell-free synthetic graft into a neoartery. Nat Med **18**: 1148-1153.

Yu J, Wang A, Tang Z, Henry J, Li-Ping Lee B, Zhu Y, Yuan F, Huang F, Li S (2012) The effect of stromal cell-derived factor-1α/heparin coating of biodegradable vascular grafts on the recruitment of both endothelial and smooth muscle progenitor cells for accelerated regeneration. Biomaterials **33**: 8062-8074.

Yokota T, Ichikawa H, Matsumiya G, Kuratani T, Sakaguchi T, Iwai S, Shirakawa Y, Torikai K, Saito A, Uchimura E, Kawaguchi N, Matsuura N, Sawa Y (2008) *In situ* tissue regeneration using a novel tissue-engineered, small-caliber vascular graft without cell seeding. J Thorac Cardiovasc Surg **136**: 900-907.

Ziche M, Morbidelli L, Pacini M, Geppetti P, Alessandri G, Maggi CA (1990) Substance P stimulates neovascularization *in vivo* and proliferation of cultured endothelial cells. Microvasc Res **40**: 264-278.

Zilla P, Preiss P, Groscurth P, Rosemeier F, Deutsch M, Odell J, Heidinger C, Fasol R, von Oppell U (1994) *In vitro*-lined endothelium: initial integrity and ultrastructural events. Surgery **116**: 524-534.

Zilla P, Bezuidenhout D, Human P (2007) Prosthetic vascular grafts: wrong models, wrong questions and no healing. Biomaterials **28**; 5009-5027.

Discussion with Reviewer

Reviewer I: The vascular scaffolds were evaluated after subcutaneous implantation, which does not reflect their future use as vascular interposition grafts. Can the authors speculate how the material properties and incorporation of SP may affect the performance of their scaffolds under flow conditions?

Authors: This is an intriguing comment and obviously an important aspect of the vascular graft development. We agreed with the reviewer's point of view that subcutaneous implantation does not accurately reflect the real interposition. Currently, we are designing a study to evaluate the potential of these scaffolds as abdominal interposition grafts in dogs. Poly(L-lactide-co-ε-caprolactone) (PLCL) (50:50) is a mechano-elastic and biodegradable copolymer. Because degradation is an essential cue for host remodelling and mechanical conditioning is recognised as an important remodelling cue for the vascular regeneration, these two key material properties may provide a conductive environment for turning an artificial vascular graft (PLCL) into a functional neo-artery *in vivo*. Previous studies from our group (Mun *et al*., 2013) and others have already proven the potential of PLCL (50:50) as an ideal vascular graft material for small-diameter blood vessel regeneration. Such grafts fostered *in situ* endothelialisation, smooth muscle cells regeneration, and neotissues formation under flow condition, and currently such cell-seeded grafts are being evaluated clinically in USA (Vogel G, Science 33; 1088-9: 2011). While *in situ* tissue regeneration is a natural process and involves the endogenous stem/progenitor cells, the small numbers of adult stem cells may not be sufficient for effective tissue regeneration. Therefore, we covalently immobilised SP with PLCL to foster tissue regeneration through the mobilisation and recruitment of stromal cells and by the promotion of angiogenesis. Since SP has abilities to mobilise and recruit mesenchymal stem cells and angiogenic cells and alter the inflammatory response (Hong *et al.,* 2009; Amadesi *et al.,* 2012), we speculate that endogenous cells (MSCs & CD34+) could be recruited to vascular grafts from the BM, circulation or adjacent vasculature because of elevation of SP gradient. These cell populations could be differentiated to vascular phenotypes because SP could provide a conductive environment for cell differentiation, proliferation, and metabolism. We hope that our future studies will clarify PLCL and SP potential for vascular regeneration.

Editor's Note: Scientific Editor in charge of the paper: Mauro Alini.